45 p.

NASA TECHNICAL NOTE

NASA TN D-1878

NASA TN D-1878

EFFECT OF VARIABLE THERMAL PROPERTIES ON ONE-DIMENSIONAL HEAT TRANSFER IN RADIATING FINS

by Norbert O. Stockman and John L. Kramer
Lewis Research Center
Cleveland, Ohio

NATIONAL AERONAUTICS AND SPACE ADMINISTRATION • WASHINGTON, D.C. • OCTOBER 1963

TECHNICAL NOTE D-1878

EFFECT OF VARIABLE THERMAL PROPERTIES ON ONE-DIMENSIONAL HEAT TRANSFER IN RADIATING FINS

By Norbert O. Stockman and John L. Kramer

Lewis Research Center
Cleveland, Ohio

NATIONAL AERONAUTICS AND SPACE ADMINISTRATION

NATIONAL AERONAUTICS AND SPACE ADMINISTRATION

TECHNICAL NOTE D-1878

EFFECT OF VARIABLE THERMAL PROPERTIES ON ONE-DIMENSIONAL HEAT TRANSFER IN RADIATING FINS

By Norbert O. Stockman and John L. Kramer

SUMMARY

An equation is derived for the temperature distribution in a rectangular fin of infinite width and of finite length and thickness that assumes one-dimensional conduction along the finite length and radiation from both sides to an equivalent sink temperature, with material emissivity and conductivity given as functions of temperature. Results in the form of a radiating effectiveness and temperature distribution are presented for several materials and surface coatings with linearly varying conductivity and emissivity. The percent error in radiating effectiveness as a result of assuming constant properties is also given for these cases. A correlation is obtained that permits simple calculation of the heat rejected by a fin of variable conductivity and variable emissivity from the readily available data for a fin with constant properties.

INTRODUCTION

Electric-power generation systems for space applications must reject large amounts of waste heat. At the present state of the art of design of such systems, the most likely method of rejecting this heat is by means of a radiator that utilizes some sort of fin-tube configuration (fig. 1). Since fins represent a portion of the radiator weight that can be minimized, it is necessary to design the fins carefully. The design procedure is usually based on one-dimensional heat-transfer calculations with constant properties to determine the temperature distribution along the fins and the effectiveness of fins in rejecting heat. A detailed analysis of such calculations for fins without tubes is given in reference 1. Similar fin calculations are used in references 2 and 3. Reference 4, although it considers the tube in its weight optimization, still uses the same fin calculation in optimizing the fin for a given tube size and material.

In many cases the temperature variation in a fin may be large, and the assumption of constant properties can be questioned. For example, a beryllium fin at a base temperature of 1800° R and optimized according to reference 4 has a temperature drop of 380° along its length. This temperature drop results in a change in conductivity from 48 Btu per hour per foot per degree Rankine at 1800° R to 59 Btu per hour per foot per degree Rankine at 1420° R, an increase of 23 percent. If this fin had a beryllium oxide coating, the emissivity would

vary from 0.72 at 1800° R to 0.75 at 1420° R, an increase of about 4 percent. To determine whether such variations as these result in significant changes in fin heat transfer (i.e., to check the validity of the assumption of constant properties), calculations of fin heat-transfer and temperature distributions that use variable conductivity and variable emissivity as functions of temperature were carried out at the NASA Lewis Research Center.

A brief analysis of the one-dimensional variable-property heat transfer in a radiating fin is presented herein. Results in the form of temperature distributions, dimensionless heat rejection (radiating effectiveness), and percent error (as a result of assuming constant properties) are obtained for several materials with various emittance coatings. For use in cases in which the error is judged to be significant, a simple correlation is given that permits calculation of the variable-property heat rejection from the readily available value of the constant-property heat rejection (e.g., ref. 1). Finally, the effect of nonzero sink temperature is considered.

ANALYSIS

The analysis is based on the assumption of one-dimensional heat conduction in unit width of a rectangular fin of infinite width and finite length and thickness radiating to an equivalent sink temperature. Although only the fin is analyzed, the boundary conditions are obtained from the relation of the fin to the adjacent tubes (fig. 1). The left edge of the fin is assumed to be at a constant temperature T_o equal to the outside tube-wall temperature. Because of symmetry about the line midway between tubes, there is no heat transfer across the midline, and only one half the fin is considered. The radiation to an equivalent sink temperature is assumed to be the same from both the top and the bottom of the fin, and radiant interchange between fin and tubes is neglected.

General Case

The one-dimensional heat balance of an elemental cross section of a rectangular fin is given by (fig. 2):

$$dQ_r = Q_x - Q_{x+dx} = Q_x - \left(Q_x + \frac{dQ_x}{dx}\,dx\right) = -\frac{dQ_x}{dx}\,dx \tag{1}$$

where Q is the heat flow per unit width. (All symbols are defined in the appendix.)

The heat radiated from such an element to an equivalent sink temperature T_s is given by

$$dQ_r = 2\epsilon(T)\sigma(T^4 - T_s^4)dx \tag{2}$$

where $\epsilon(T)$ is the emissivity as a function of temperature.

The heat conducted into the element is

$$Q_x = -k(T)t \frac{dT}{dx}$$

where $k(T)$ is the conductivity as a function of temperature.

The rate of change of the heat conducted with respect to distance is

$$\frac{dQ_x}{dx} = -t\left[k(T) \frac{d^2T}{dx^2} + \frac{dT}{dx} \frac{dk(T)}{dx}\right] \tag{3}$$

but

$$\frac{dk(T)}{dx} = \frac{dk(T)}{dT} \frac{dT}{dx}$$

since $k(T)$ is a function of T only. Combining this relation and equations (1) to (3) gives

$$\frac{d^2T}{dx^2} = \frac{2\epsilon(T)\sigma(T^4 - T_s^4)}{tk(T)} - \frac{1}{k(T)} \frac{dk(T)}{dT} \left(\frac{dT}{dx}\right)^2 \tag{4}$$

This equation together with the boundary conditions $T = T_o$ at $x = 0$ and $dT/dx = 0$ at $x = l$ determines the one-dimensional temperature distribution in a rectangular fin.

Equation (4) can be made nondimensional by the following transformations:

$$\theta = T/T_o$$

$$X = x/l$$

$$\lambda = \frac{2\sigma\epsilon(T_o)l^2T_o^3}{k(T_o)t}$$

$$K(\theta) = \frac{k(T)}{k(T_o)}$$

$$M(\theta) = \frac{\epsilon(T)}{\epsilon(T_o)}$$

which result in

$$\frac{d^2\theta}{dX^2} = \frac{\lambda M(\theta)}{K(\theta)} (\theta^4 - \theta_s^4) - \frac{1}{K(\theta)} \frac{dK(\theta)}{d\theta} \left(\frac{d\theta}{dX}\right)^2 \tag{5}$$

The boundary conditions become $\theta = 1.0$ at $X = 0$ and $d\theta/dX = 0$ at $X = 1.0$.

From equation (5), it can be seen that the temperature distribution along the fin depends on λ, θ_s, $K(\theta)$, and $M(\theta)$, where the functions $K(\theta)$ and $M(\theta)$ (or $k(T)$ and $\epsilon(T)$) may be any functions that fit the empirical emissivity and conductivity data. For constant properties, $M(\theta) = 1.0$, $K(\theta) = 1.0$, $dK(\theta)/d\theta = 0$, and the temperature distribution depends only on λ and θ_s.

Linear Variations

In many cases, conductivity and emissivity data can be sufficiently well represented by straight-line variations. Specifically, the emissivity function is then given by

$$M(\theta) = A + B\theta \tag{6}$$

This can be put into a more informative form by noting that

$$M(\theta) = 1 + M'(\theta - 1) \tag{7}$$

where

$$M' = \frac{dM(\theta)}{d\theta}$$

Similarly, the conductivity function can be written

$$K(\theta) = 1 + K'(\theta - 1) \tag{8}$$

where

$$K' = \frac{dK(\theta)}{d\theta}$$

Putting equations (7) and (8) into equation (5) gives

$$\frac{d^2\theta}{dX^2} = \frac{\lambda[1 + M'(\theta - 1)]}{[1 + K'(\theta - 1)]}(\theta^4 - \theta_s^4) - \frac{1}{[1 + K'(\theta - 1)]} K' \left(\frac{d\theta}{dX}\right)^2 \tag{9}$$

It can be seen from equation (9), therefore, that for linearly varying k and ϵ the temperature distribution along the fin depends on λ, θ_s, and the slopes M' and K' of the variable-property functions.

Fin Effectiveness

A common measure of fin performance is the radiating effectiveness η, which is defined as the ratio of the heat radiated by the fin based on the calculated temperature distribution to the heat radiated by the fin at base temperature T_o throughout; that is,

$$\eta = \frac{\int_0^l \epsilon(T)\sigma(T^4 - T_s^4)\,dX}{\epsilon(T_o)\sigma(T_o^4 - T_s^4)\,l} = \frac{\int_0^1 M(\theta^4 - \theta_s^4)dX}{1 - \theta_s^4} \tag{10}$$

This is a nondimensional heat rejection, and the actual heat rejected per unit width Q by a given fin can be computed from it by

$$Q = \eta l \epsilon \sigma (T_o^4 - T_s^4) \tag{11}$$

A measure of the effect of assuming constant properties in computing η (or Q) of a given fin for a given λ and θ_s is the percent error E_v, which is defined for simplicity as

$$E_v = 100\left(1 - \frac{\eta_v}{\eta_c}\right) \tag{12}$$

where η_c is the effectiveness obtained for constant properties, and η_v is the effectiveness obtained from the variable-properties solution (eq. (5) or (9)). Constant-property results can be obtained from reference 1 or by solving equation (9) with $K' = 0$ and $M' = 0$, or equation (5) with $M(\theta) = 1.0$, $K(\theta) = 1.0$, and $K' = 0$.

Method of Solution

Equation (9) was solved for θ numerically by using a Runge-Kutta method on a high-speed digital computer. An estimate of the midfin temperature ratio θ_l was required to start the iterative procedure. Since an arbitrary guess for θ_l was not sufficient to ensure convergence, the constant-property value from reference 1 was used and was sufficient for all cases treated herein.

Equation (10) was integrated numerically to obtain η. As a check on the entire method, η was also calculated from the Fourier relation for conduction at the base of the fin:

$$\eta = \frac{-\left(\frac{d\theta}{dX}\right)_o}{\lambda\left(1 - \theta_s^4\right)}$$

In all cases, the values of η computed from both methods agreed to five places.

RESULTS

Inputs

Nondimensional conductivity variations for materials of possible interest

for fins of fin-tube radiators are shown in figure 3 and table I. Nondimensional emissivity variations are shown in figure 4 and table I. These variations are for two coatings at each of three temperatures plus two extreme hypothetical cases created to give a range of variation similar to that of the variable conductivity. Except for the hypothetical cases, the curves of figures 3 and 4 are based on empirical data gathered from many sources in the literature.

Solutions for θ, η, and E_v were obtained for the illustrative property distributions of figures 3 and 4 for a range of values of λ from 0.25 to 5.0. In all cases, the property variations are identified by their respective slopes K' and M' (table I). Constant-property values were obtained from the equations developed herein for $M' = 0$ and $K' = 0$. The effect of variable conductivity is first presented by comparing results of variable conductivity and constant emissivity with those of constant conductivity and constant emissivity for zero sink temperature. Next, the effect of variable emissivity is considered in a similar manner. Then the combined effect of variable conductivity and variable emissivity is studied by comparing results with those of constant-property solutions. Finally, the effect of nonzero sink temperature is briefly considered.

Effect of Variable Conductivity

Variations. - Radiating effectiveness η is plotted against λ in figure 5 for the constant-property case and two selected variable-conductivity cases (constant emissivity) as indicated. When the conductivity slope K' is positive (case F in fig. 5), η_K is less than the constant property η_c. Since the conductivity is decreasing with temperature along the fin, less heat is conducted and therefore less is radiated. Conversely, when K' is negative (case B in fig. 5), η_K is greater than η_c. These effects hold for all values of λ, but the magnitude of the effect increases with λ.

The temperature ratio θ_l on a fin at a location midway between tubes represents the lowest temperature in a fin-tube radiator and is shown in figure 6 as a function of λ. Here, the same type of effect is noted as in figure 5: Since less heat is conducted, less is radiated; therefore, the temperatures on the fin must be lower than those of the constant-property case.

Since the entire temperature distribution along the fin may be of interest, the temperature ratio is shown in figure 7 as a function of distance ratio along the fin (from base to midpoint) for three values of λ.

Error. - Figure 8 shows the variation in percent error in η_K with λ for the variable-conductivity cases considered in figure 3. An initial rapid increase in error with increasing λ is seen in all cases. For a design value of λ of 0.9, as is generally obtained from weight minimization studies (ref. 4), the error is less than 4 percent. A summary of the percent error and other results is given in table II.

Correlation. - It was also observed that η_K varied essentially linearly

with conductivity slope K', as shown in figure 9. For a given λ, the points lie very nearly on the least-squares straight line of the form

$$\eta_K^* = \eta_c + \alpha K' \tag{13}$$

where the superscript $*$ indicates that η_K^* has been obtained from the correlation rather than from the specific equation solution, and α is a function of λ, as given in figure 10. This means that a good approximation to η_K with variable conductivity assumed can be obtained from the slope of the linear conductivity function, the constant property η_c, and the coefficient α. In table II, η_K^* is given for several cases for comparison with the exact value η_K.

If equation (13) is used in equation (12), a good approximation E_K^* to the percent error E_K is obtained in the form

$$E_K^* = -100 \frac{\alpha K'}{\eta_c} \tag{14}$$

Thus, in the engineering use of the data, equation (14) in conjunction with figure 10 for α and figure 5 for η_c can be used to determine whether the material (K') and geometry (λ) of interest result in a significant error. If they do, the corrected fin effectiveness η_c^* can be calculated from equation (13).

Effect of Variable Emissivity

Variations. - Radiating effectiveness η is plotted against λ in figure 11 for the constant-property case and several variable-emissivity cases (constant conductivity), as indicated. Here, the effect is similar to that of variable conductivity, that is, the higher the emissivity slope M' the lower the radiating effectiveness. This is to be expected in view of the reduced fin radiation as emissivity decreases with decreasing temperature along the fin.

The midfin temperature ratio θ_l is plotted in figure 12 as a function of λ. Here, the effect is the reverse of that noted for figure 11. This effect is explained as follows for the case with positive M': The reduction in heat radiated compared to the case of constant emissivity results in less heat conducted, which, in turn, results in a smaller temperature gradient. This effect is confirmed in figure 13 where the temperature ratio θ is plotted against distance ratio X for $\lambda = 0.5$, 0.9, and 5.0. The temperature ratio for the positive M' case is everywhere greater than that for the constant-property case.

Error. - Figure 14 shows the variation in percent error E_M in η_M with λ for the variable-emissivity cases considered in figure 4. Comparing this with figure 8 (E_K against λ) points out three things: E_M changes more rapidly with λ than E_K at small values of λ; E_M levels off at smaller values of λ; and, for values of M' comparable to values of K', the magnitude of E_M is

greater than that of E_K, especially at small values of λ. Figure 14 also shows that significant error (up to about 10 percent) can be obtained for weight-optimized designs with $\lambda = 0.9$ for the extreme case. However, for realistic materials and surface coatings or conditions, the absolute value of the emissivity slope is usually smaller than that of the material conductivity slope.

Calculating the net heat transfer from radiators with high emissivity coatings shows that another source of error in addition to the temperature variation of the emissivity may be in the relatively poor conductivity of the coatings. This topic is treated in reference 5, where it is pointed out that the error in fin efficiency that results from neglecting the thickness of the coating may be significant for space radiator-design calculation.

Correlation. - As in the conductivity case, it was observed that η_M varied essentially linearly with emissivity slope M', as shown in figure 15. For a given λ, the points lie very nearly on the least-squares straight line of the form

$$\eta_M^* = \eta_c + \beta M' \tag{15}$$

where β is a function of λ, as given in figure 16. Equation (15) can be used to obtain a good approximation to the variable-emissivity radiating effectiveness from the slope of the linear emissivity function, the constant property η_c, and the coefficient β. The η_M^* for several cases and a summary of the previous results are presented in table III.

If equation (15) is used in equation (12), the approximate error E_M^* is obtained as

$$E_M^* = - \frac{100\ \beta M'}{\eta_c} \tag{16}$$

Equation (16) in conjunction with figure 16 for β and figure 5 for η_c can be used to determine whether the emissivity variation M' and the fin geometry λ of interest result in a significant error. If so, the corrected fin effectiveness η_M^* can be calculated from equation (15).

Effect of Variable Conductivity and Variable Emissivity

Variations. - The radiating effectiveness η for four cases of combined variable conductivity and emissivity and for that of the constant-property case is plotted against λ in figure 17. The curve for $K' = -1.267$, $M' = -1.500$ is much higher than the constant-property curve because both K' and M' are negative and tend to increase η. The $K' = 0.482$, $M' = 0.500$ curve is lower than the constant-property curve because both K' and M' are positive and tend to decrease η. The curve $K' = 0.482$, $M' = -1.500$ is higher than the

constant-property curve even though K' here tends to decrease η because, in this case, the magnitude of M' is greater than that of K' and because, in general, a given value of M' produces a greater effect than a comparable value of K'. The curve $K' = -1.267$, $M' = 0.500$ is very close to the constant-property curve because the effects of K' and M' very nearly cancel. In this case, for λ less than about 1.2, the effect of M' predominates and $\eta_{K,M}$ is less than η_c. For λ greater than 1.2, K' takes over and $\eta_{K,M}$ is greater than η_c.

In figure 18, the midfin temperature ratio θ_l is plotted against λ. Curve $K' = -1.267$, $M' = 0.500$ is considerably higher than the constant-property curve because K' and M' both tend to increase θ_l. Curve $K' = 0.482$, $M' = -1.500$ is considerably lower because K' and M' both tend to decrease θ_l. The other two curves are relatively close to the constant-property curve because, in both cases, K' and M' have opposite effects that tend to cancel, although, in both cases, the effect of M' predominates.

The temperature ratio is plotted in figure 19 against distance ratio along the fin. The same comments made about figure 18 also apply to this figure.

Error. - The percent error $E_{K,M}$ in $\eta_{K,M}$ is shown in figure 20 where $E_{K,M}$ is plotted against λ for each pair of K' and M'. These curves are not, in general, as simple as the error curves for variable conductivity only or variable emissivity only because of the relative effects of the two factors.

It can be seen in figure 20 that, even for small values of λ, the error can be substantial in cases where K' and M' are of the same sign and of relatively large magnitude.

Correlation. - In addition to the four cases just discussed, solutions of equation (9) were obtained for several other combinations of K' and M', and the radiating effectiveness $\eta_{K,M}$ for all cases was computed. After comparison of these results with the results of variable conductivity only and variable emissivity only, it was observed that $\eta_{K,M}$ varied essentially linearly with $\alpha K' + \beta M'$, as shown in figure 21. For a given λ, the points lie very nearly on a straight line of the form

$$\eta^*_{K,M} = \eta_c + \alpha K' + \beta M' \tag{17}$$

The agreement between lines and data points is good for small values of λ, but some points deviate from the curves for larger values of λ. Equation (17) can be used to obtain a good approximation to $\eta_{K,M}$ for both conductivity and emissivity variable from the constant property η_c, the prescribed K' and M', and the coefficients α (fig. 10) and β (fig. 16). Note that equation (17) reduces to equation (13) when emissivity is constant and to equation (15) when conductivity is constant. The $\eta^*_{K,M}$ for several cases and a summary of the previous results are presented in table IV.

If equation (17) is used in equation (12), a good approximation $E^*_{K,M}$ to the percent error $E_{K,M}$ is obtained in the form

$$E^*_{K,M} = -\frac{100}{\eta_c}(\alpha K' + \beta M') \tag{18}$$

In comparing equation (18) with equations (14) and (16), it can be seen that $E^*_{K,M} = E^*_K + E^*_M$; that is, the separate effects of variable conductivity and variable emissivity combine additively to produce the effect of both properties variable.

In the engineering use of the data presented in this section, equation (18) in conjunction with figure 10 for α, figure 16 for β, and figure 5 for η_c can be used to determine whether the material (K'), coating (M'), and geometry (λ) of interest result in a significant error. If they do, the corrected fin effectiveness $\eta^*_{K,M}$ can be calculated from equation (17).

Effect of Nonzero Sink Temperature

To investigate the effect of nonzero sink temperature on the usefulness of the results presented, the percent error was obtained for several cases (values of K' and M') for a range of values of sink temperature θ_s. Results are shown in figure 22 for a λ of 0.9, which is the currently used optimum value. In all cases, it can be seen that the percent error is essentially constant up to values of θ_s of about 0.3. Since a realistic sink temperature ratio in general, will not be above 0.3, the zero sink temperature results should be applicable in most practical cases.

CONCLUDING REMARKS

A study has been made of the effects on fin radiating effectiveness and midfin and local temperature ratios of assuming one or both of conductivity and emissivity to be linear functions of temperature, characterized by their slopes. A percent error was defined for evaluating the deviation of the constant-property radiating effectiveness from the more realistic variable-property radiating effectiveness. The principal results obtained are as follows:

1. At an optimum geometric parameter value of 0.9 and at zero sink temperature, the error in neglecting conductivity variation is probably not significant; the largest error for the materials investigated was around 3 percent for beryllium at 1900° R and pyrolytic graphite at 2400° R. The error in neglecting emissivity variation was small in most of the realistic coatings considered but reached almost 9 percent for aluminum oxide at 2400° R. The combined effect of neglecting both conductivity and emissivity variations may be quite significant when the conductivity and emissivity slopes are relatively large and of the same sign. For example, the error for aluminum oxide (emissivity slope = -1.165) on pyrolytic graphite (conductivity slope = -1.409) at 2400° R would be about 12 percent.

2. The percent error increases with geometric parameter except in cases where the conductivity and emissivity slopes are of opposite sign.

3. The percent error remains essentially constant as sink temperature ratio increases from zero to about 0.3, and then decreases rather rapidly as the ratio approaches 1.0.

4. A linear correlation was obtained between the radiating effectiveness and the conductivity and emissivity slopes as a function of the geometric parameter. This correlation permitted the rapid calculation of approximate percent error and radiating effectiveness for preliminary design purposes.

Lewis Research Center
National Aeronautics and Space Administration
Cleveland, Ohio, May 13, 1963

APPENDIX - SYMBOLS

A,B	coefficients in emissivity function (eq. (6))
E	percent error of constant-property radiating effectiveness (eq. (12))
K	conductivity ratio, $k(T)/k(T_o)$
K'	conductivity slope, $dK(\theta)/d\theta$
k	conductivity, Btu/(hr)(ft)(^oR)
l	fin half-length, ft
M	emissivity ratio, $\epsilon(T)/\epsilon(T_o)$
M'	emissivity slope, $dM(\theta)/d\theta$
Q	heat flow per unit width, Btu/(hr)(ft)
T	temperature, ^oR
t	fin thickness, ft
X	distance ratio, x/l
x	distance from base of fin, ft
α	coefficient in radiating effectiveness - conductivity correlation (eq. (13))
β	coefficient in radiating effectiveness - emissivity correlation (eq. (15))
ϵ	emissivity
η	radiating effectiveness (eq. (10))
θ	temperature ratio, T/T_o
λ	geometric parameter, $2\sigma\epsilon(T_o)l^2T_o^3/k(T_o)t$
σ	Stefan-Boltzmann constant, 1.713×10^{-9} Btu/(hr)(ft^2)($^oR^4$)

Subscripts:

c	constant property
K	variable conductivity
l	midfin location ($x = l$)
M	variable emissivity

o fin-base location ($x = 0$)

r radiated

s sink

v variable property (may be K or M or both)

Superscript:

$*$ computed from correlation

REFERENCES

1. Lieblein, Seymour: Analysis of Temperature Distribution and Radiant Heat Transfer Along a Rectangular Fin of Constant Thickness. NASA TN D-196, 1959.

2. Bartas, J. G., and Sellers, W. H.: Radiation Fin Effectiveness. Jour. Heat Transfer (Trans. ASME), ser. C, vol. 82, no. 1, Feb. 1960, pp. 73-75.

3. Mackay, D. B., and Bacha, C. P.: Space Radiator Analysis and Design. TR 61-30, pt. I, Aero. Systems Div., Apr. 1, 1961, pp. 11-22.

4. Schreiber, L. H., Mitchell, R. P., Gillespie, G. D., and Olcott, T. M.: Techniques for Optimization of a Finned-Tube Radiator. Paper 61-SA-44, ASME, 1961.

5. Plamondon, J. A.: Thermal Efficiency of Coated Fins. Paper 61-WA-168, ASME, 1961.

TABLE I. - PROPERTY VARIATIONS

(a) Material conductivity (fig. 3)

Case	Material	Temperature, T_o, °R	Slope, K'
A	Pyrolytic graphite	2400	-1.409
B	Beryllium	1900	-1.267
C	Pyrolytic graphite	1900	-.863
D	Molybdenum	2400	-.334
E	Columbium	2400	.373
F	Aluminum	1260	.482

(b) Coating emissivity (fig. 4)

Case	Coating	Temperature, T_o, °R	Slope, M'
A	Hypothetical	----	-1.500
B	Aluminum oxide	2400	-1.165
C	Aluminum oxide	1900	-.742
D	Aluminum oxide	1260	-.394
E	Beryllium oxide	2400	-.284
F	Beryllium oxide	1900	-.213
G	Beryllium oxide	1260	-.132
H	Hypothetical	----	.500

TABLE II. - SUMMARY OF VARIABLE-CONDUCTIVITY DATA

Geometric parameter, λ	Constant property radiating effectiveness, η_c	Case	Dimensionless conductivity slope, K'	Midfin temperature ratio, θ_l	Radiating effectiveness, η_K	Percent error (eq. (12)), E_K	Radiating effectiveness from eq. (13), η_K^*
0.5	0.6634	A	-1.4094	0.8614	0.6764	-1.95	0.6768
		B	-1.2672	.8606	.6752	-1.77	.6755
		C	-.8625	.8582	.6716	-1.24	.6716
		D	-.3340	.8547	.6667	-0.50	.6666
		E	.3731	.8494	.6596	0.58	.6599
		F	.4819	.8486	.6584	0.76	.6589
0.9	0.5538	A	-1.4094	0.8065	0.5719	-3.28	0.5727
		B	-1.2672	.8052	.5703	-2.98	.5707
		C	-.8625	.8011	.5653	-2.09	.5653
		D	-.3340	.7953	.5584	-0.84	.5582
		E	.3731	.7861	.5482	1.00	.5488
		F	.4819	.7845	.5466	1.30	.5473
5.0	0.2738	A	-1.4094	0.6123	0.2952	-7.84	0.2960
		B	-1.2672	.6093	.2932	-7.12	.2938
		C	-.8625	.6001	.2874	-4.98	.2874
		D	-.3340	.5861	.2792	-2.00	.2790
		E	.3731	.5618	.2673	2.37	.2679
		F	.4819	.5572	.2653	3.09	.2661

TABLE III. - SUMMARY OF VARIABLE-EMISSIVITY DATA

Geometric parameter, λ	Constant property radiating effectiveness, η_c	Case	Dimensionless emissivity slope, M'	Midfin temperature ratio, θ_l	Radiating effectiveness, η_M	Percent error (eq. (12)), E_M	Radiating effectiveness from eq. (15), η_M^*
0.5	0.6634	A	-1.5000	0.8341	0.7276	-9.67	0.7266
		B	-1.1650	.8383	.7126	-7.42	.7125
		C	-.7422	.8435	.6943	-4.65	.6947
		D	-.3937	.8477	.6796	-2.43	.6800
		E	-.2845	.8490	.6750	-1.75	.6754
		F	-.2126	.8499	.6721	-1.30	.6724
		G	-.1316	.8508	.6688	-.80	.6690
		H	.5000	.8580	.6437	2.98	.6424
0.9	0.5538	A	-1.5000	0.7612	0.6162	-11.28	0.6155
		B	-1.1650	.7679	.6019	-8.69	.6017
		C	-.7422	.7764	.5841	-5.47	.5843
		D	-.3937	.7834	.5697	-2.87	.5700
		E	-.2845	.7856	.5652	-2.07	.5655
		F	-.2126	.7870	.5623	-1.54	.5625
		G	-.1316	.7886	.5590	-.95	.5592
		H	.5000	.8008	.5342	3.54	.5332
5.0	0.2738	A	-1.5000	0.5159	0.3075	-12.34	0.3078
		B	-1.1650	.5278	.3002	-9.66	.3002
		C	-.7422	.5439	.2908	-6.21	.2906
		D	-.3937	.5582	.2828	-3.32	.2827
		E	-.2845	.5629	.2803	-2.40	.2802
		F	-.2126	.5661	.2787	-1.80	.2786
		G	-.1316	.5697	.2768	-1.11	.2767
		H	.5000	.5994	.2621	4.26	.2624

TABLE IV. - SUMMARY OF VARIABLE-CONDUCTIVITY AND -EMISSIVITY DATA

Geometric parameter, λ	Constant property radiating effectiveness, η_c	Dimensionless conductivity slope, K'	Dimensionless emissivity slope, M'	Midfin temperature ratio, θ_l	Radiating effectiveness, $\eta_{K,M}$	Percent error, $E_{K,M}$	Radiating effectiveness from eq. (17), $\eta^*_{K,M}$
0.5	0.6634	-1.2672	-1.5	0.8449	0.7405	-11.62	0.7386
		-1.2672	.5	.8656	.6551	1.25	.6544
		.4819	-1.5	.8290	.7219	-8.82	.7220
		.4819	.5	.8546	.6388	3.71	.6378
0.9	0.5538	-1.2672	-1.5	0.7796	0.6362	-14.88	0.6325
		-1.2672	.5	.8134	.5497	.74	.5502
		.4819	-1.5	.7520	.6072	-9.64	.6091
		.4819	.5	.7949	.5275	4.75	.5268
5.0	0.2738	-1.2672	-1.5	0.5566	0.3334	-21.77	0.3279
		-1.2672	.5	.6298	.2796	-2.12	.2825
		.4819	-1.5	.4930	.2961	-8.14	.3002
		.4819	.5	.5831	.2547	6.98	.2548

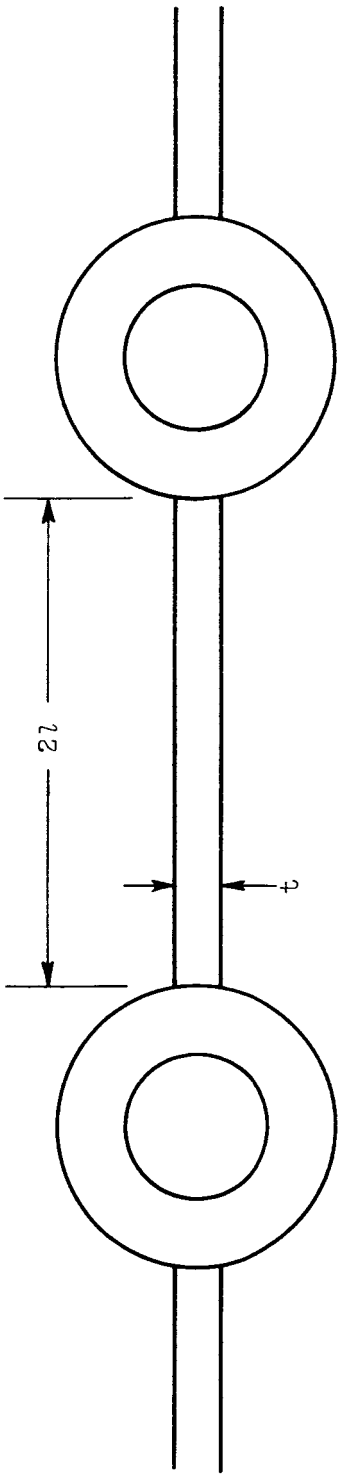

Figure 1. - Cross section of fin-tube radiator configuration.

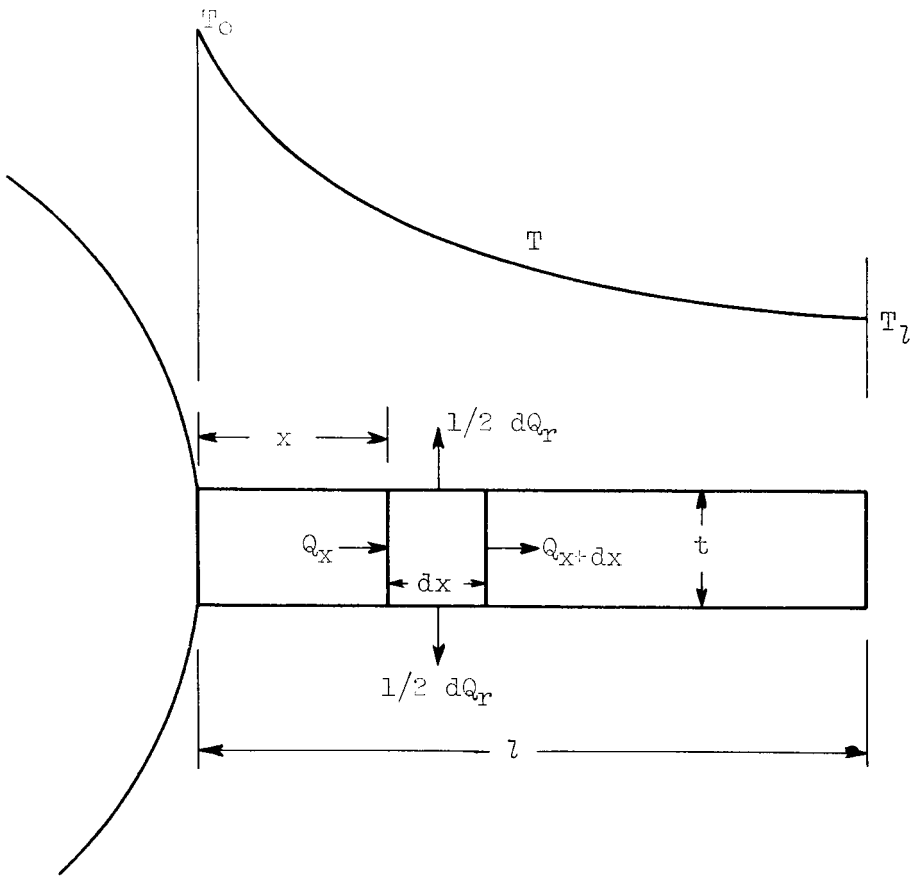

Figure 2. - Cross section of fin showing heat balance and temperature profile.

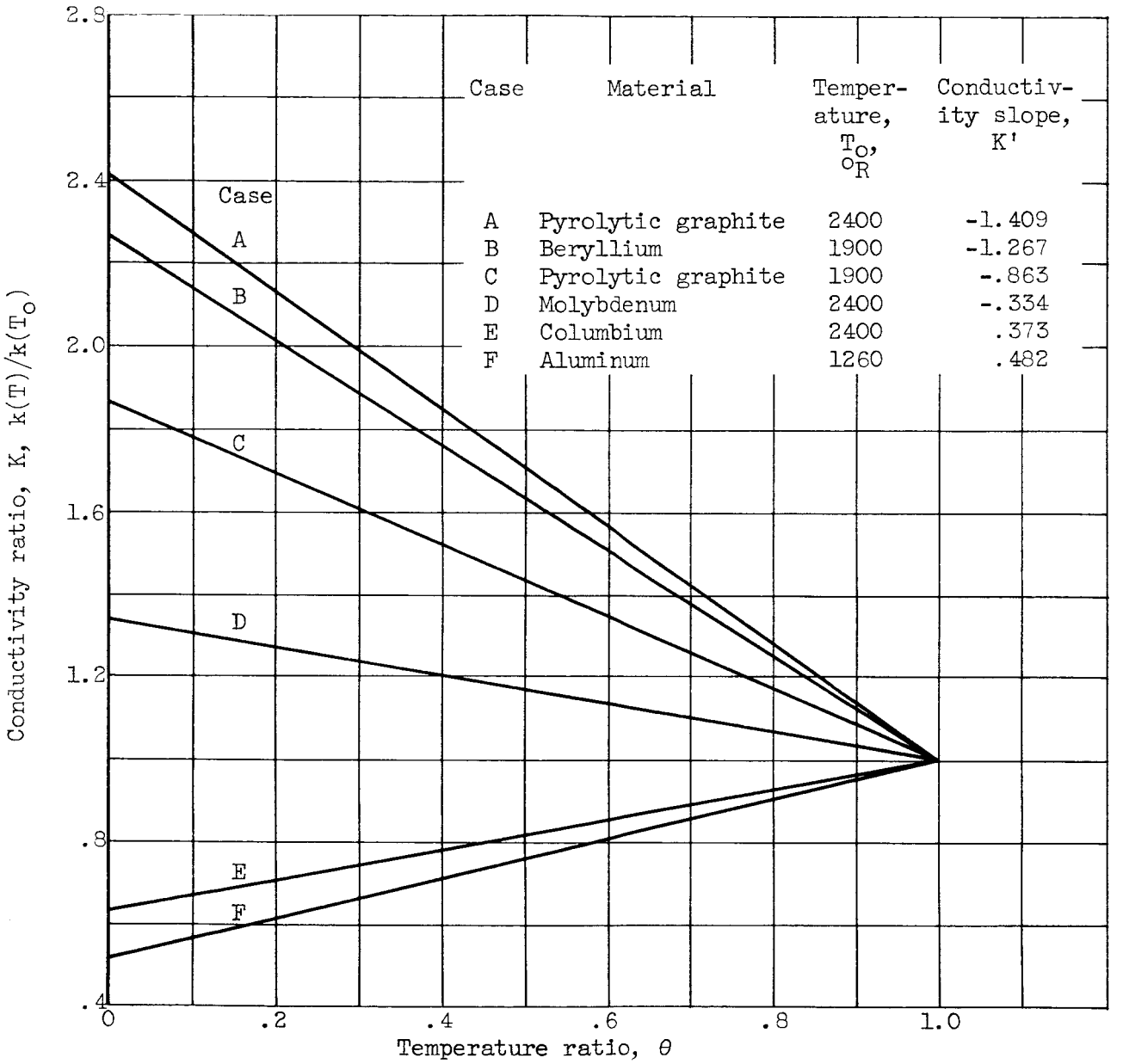

Figure 3. - Variation of conductivity ratio with temperature ratio for several materials.

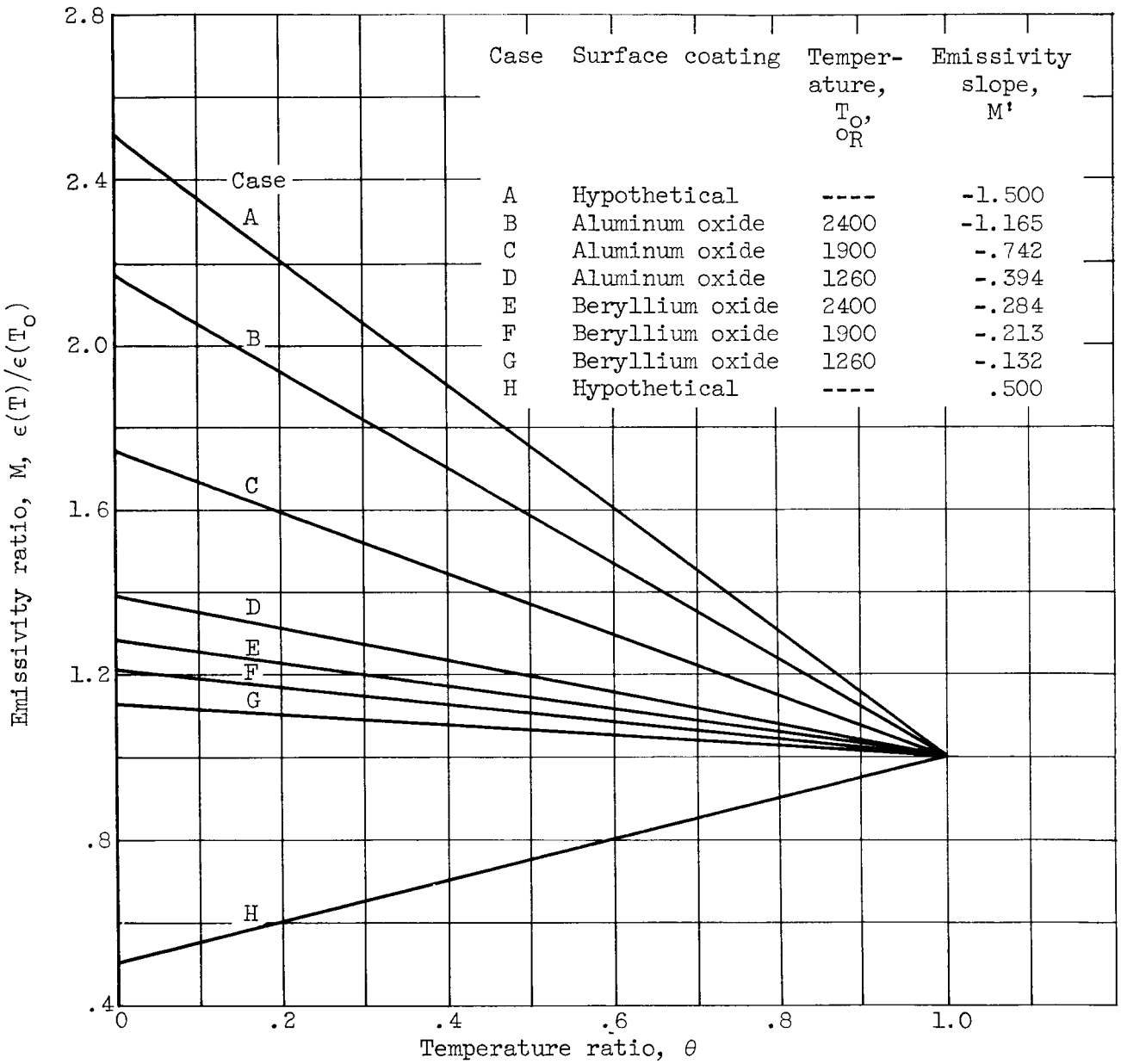

Figure 4. - Variation of emissivity ratio with temperature ratio for several surface coatings.

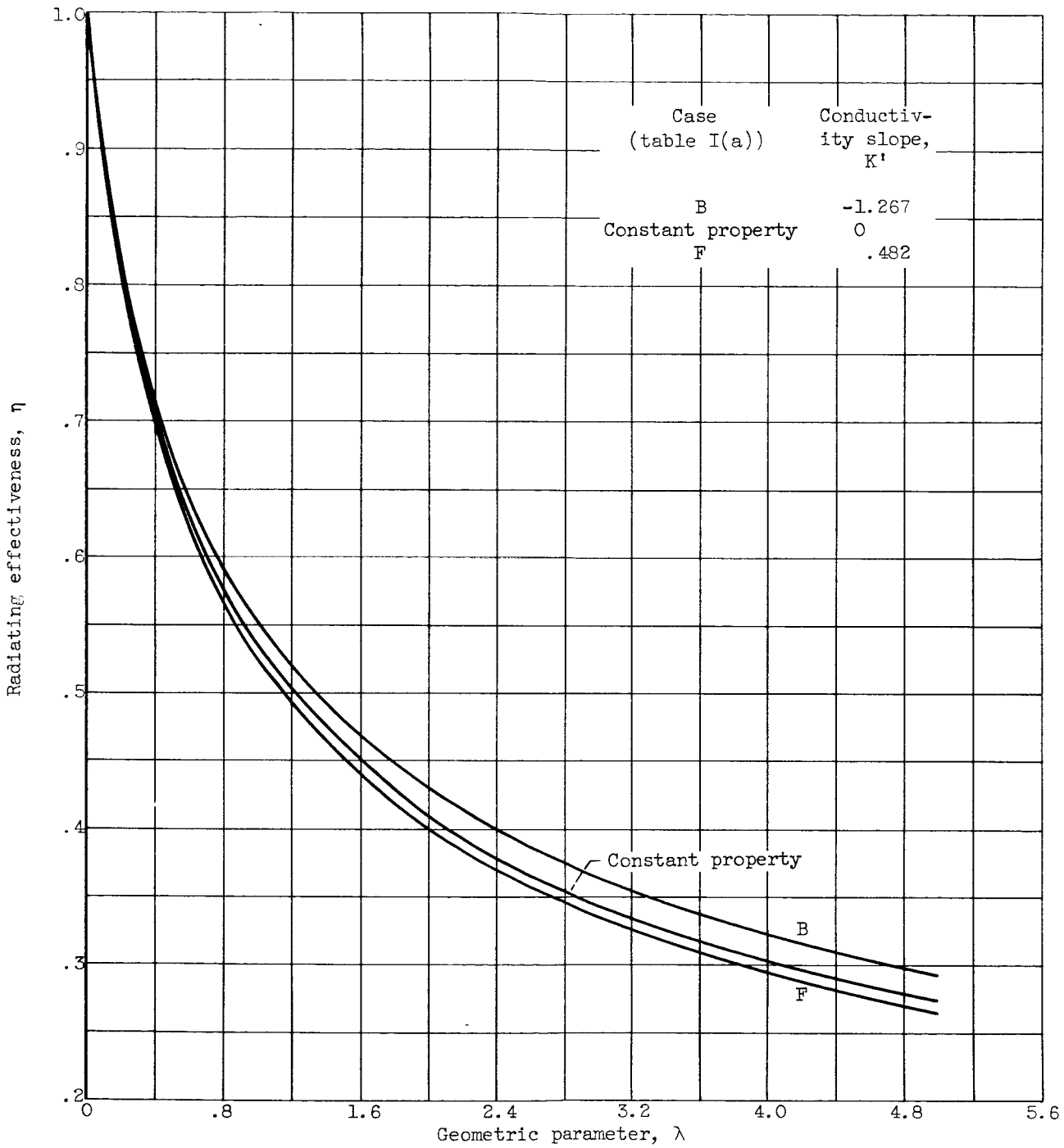

Figure 5. - Effect of variable conductivity on radiating effectiveness.

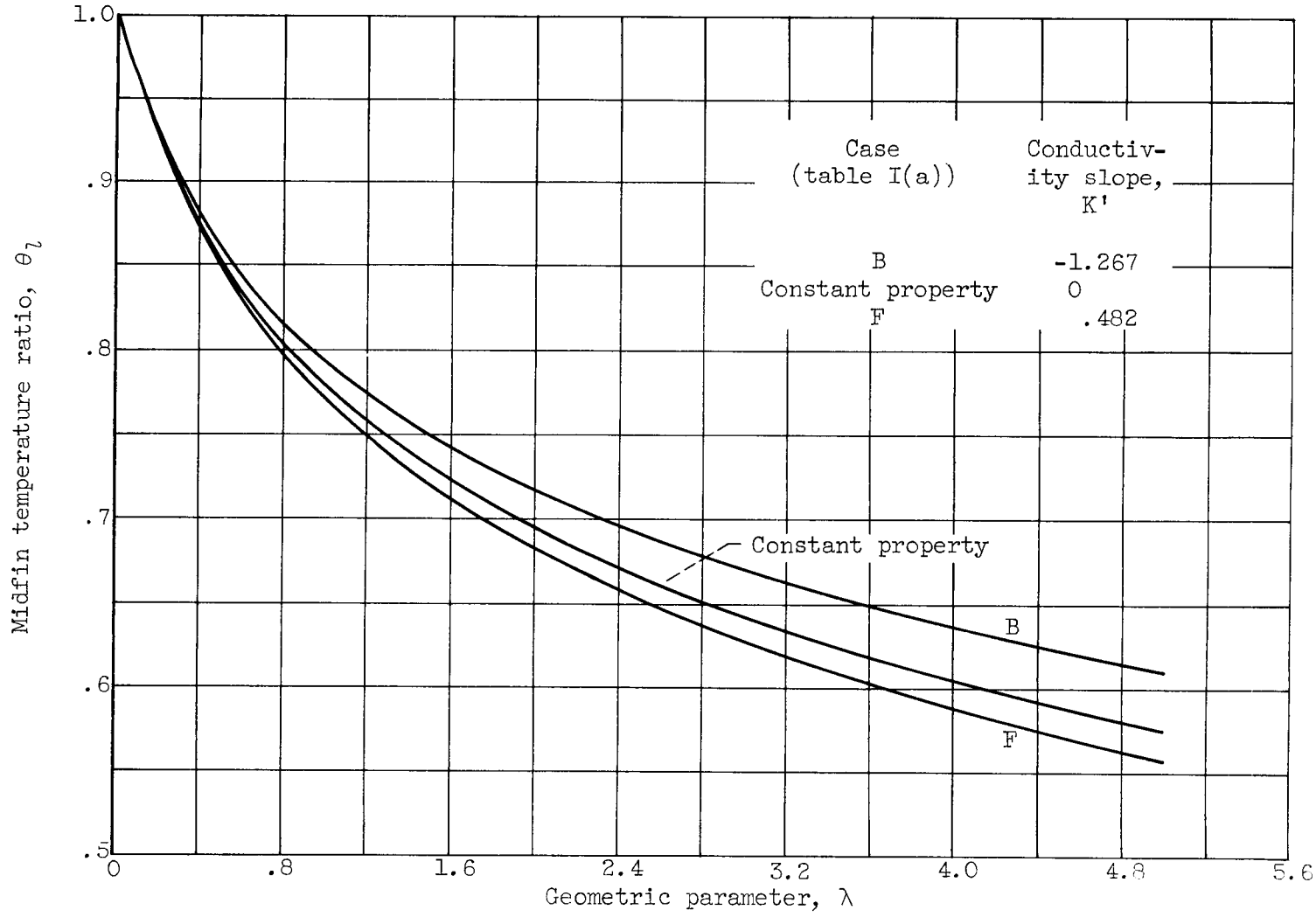

Figure 6. - Effect of variable conductivity on midfin temperature ratio.

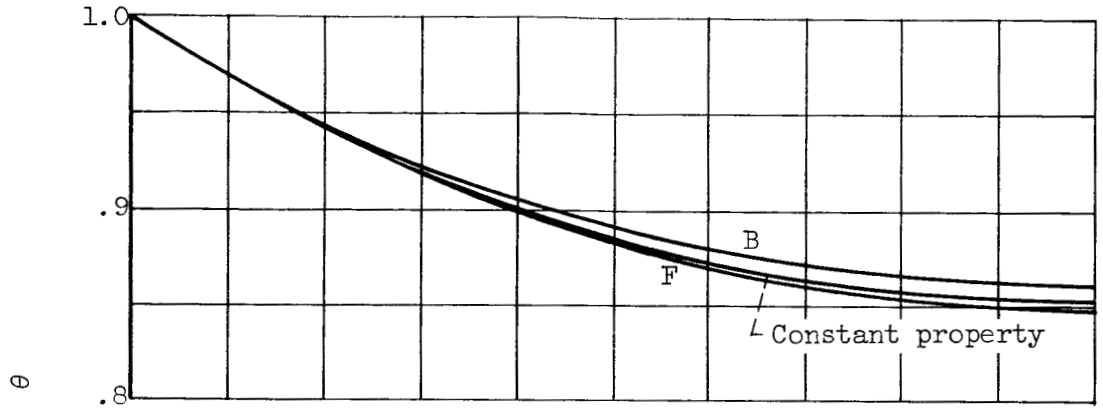

(a) Geometric parameter, λ, 0.5.

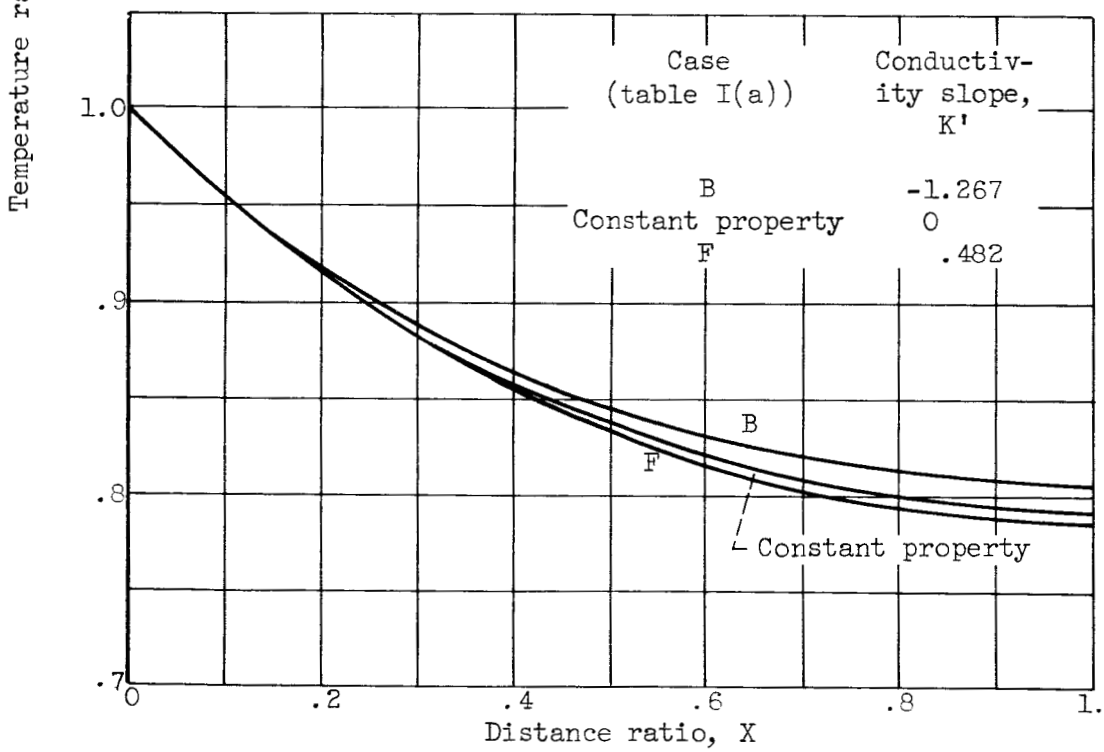

(b) Geometric parameter, λ, 0.9.

Figure 7. - Effect of variable conductivity on local temperature ratio.

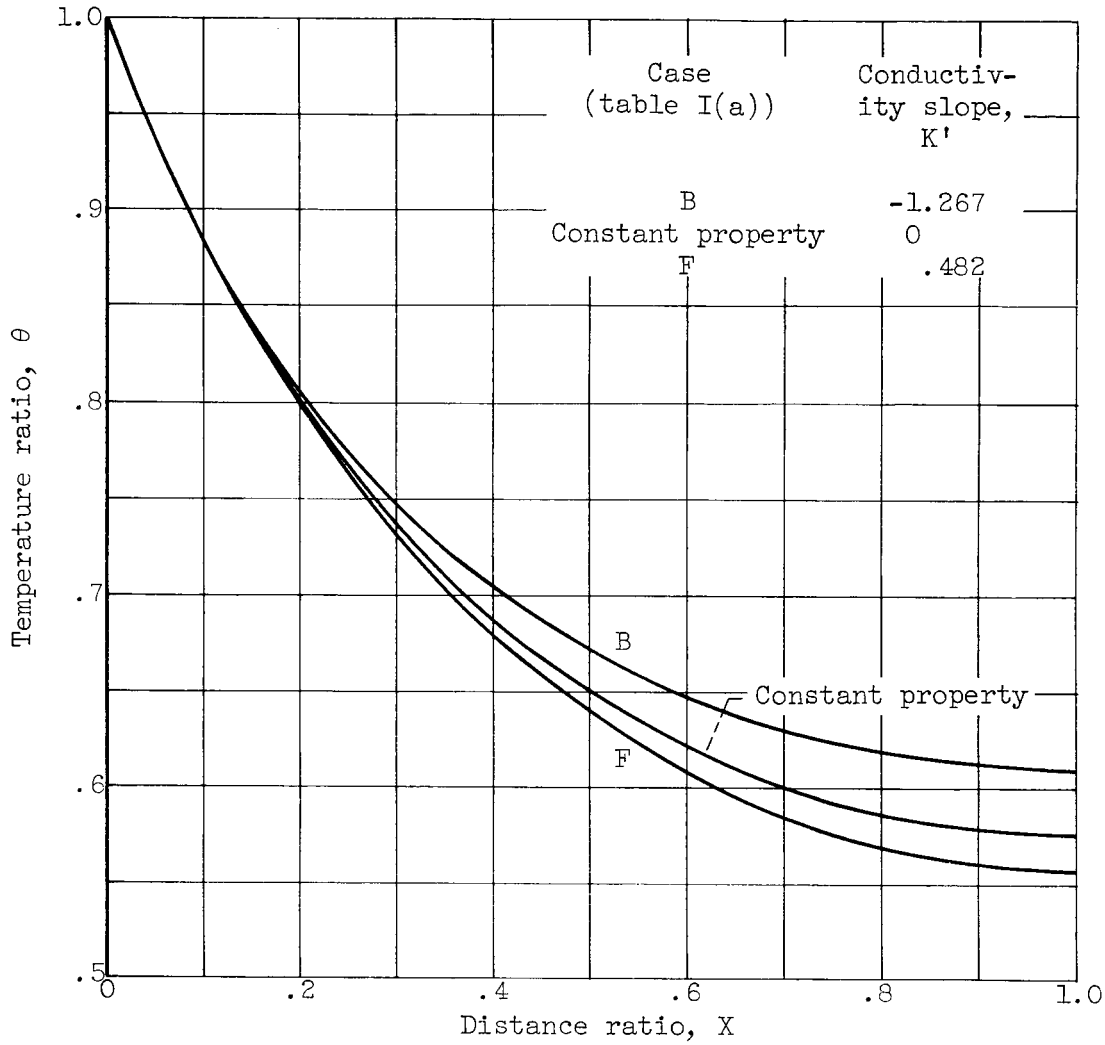

(c) Geometric parameter, λ, 5.0.

Figure 7. - Concluded. Effect of variable conductivity on local temperature ratio.

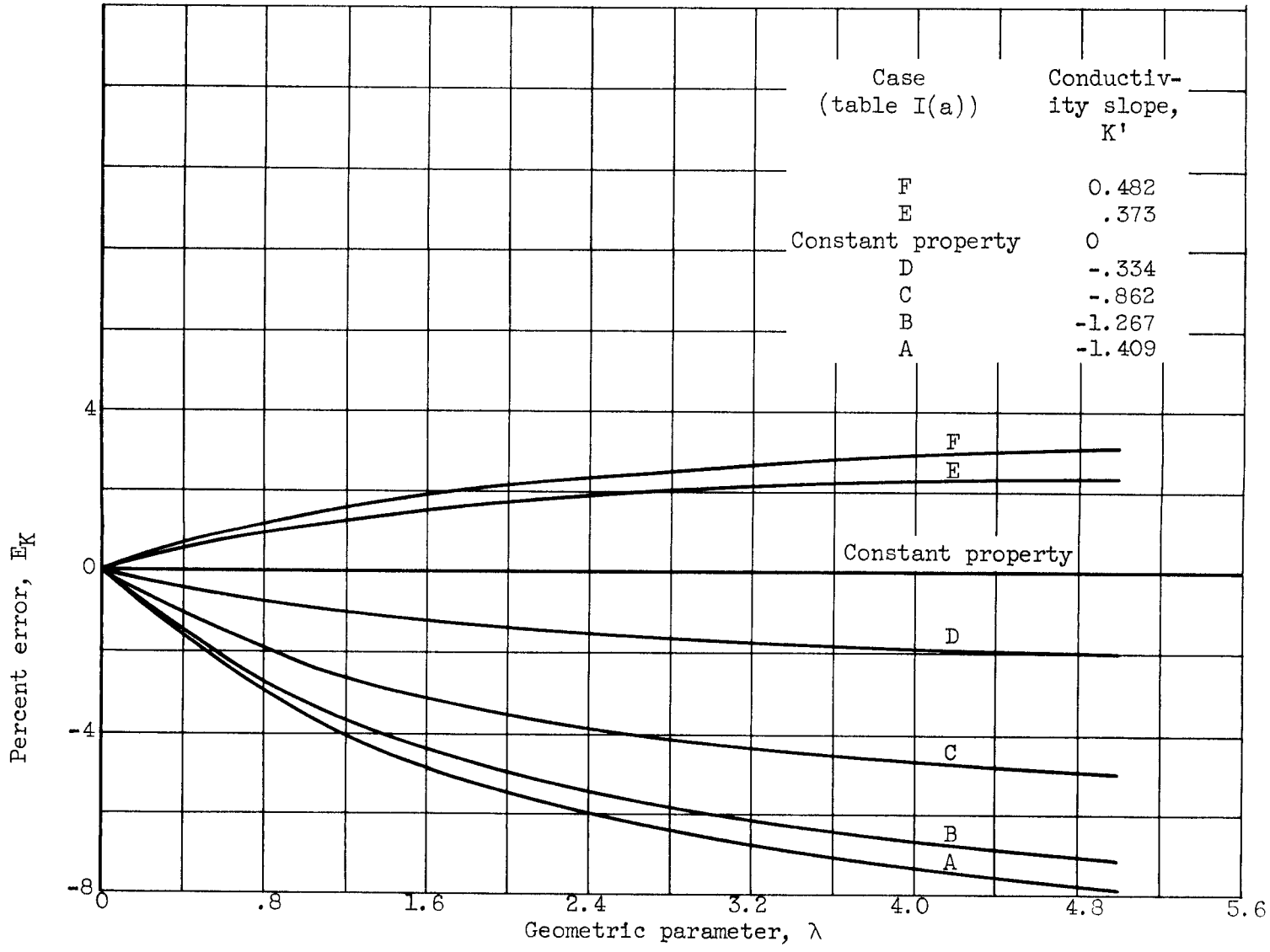

Figure 8. - Percent error in fin effectiveness for variable conductivity.

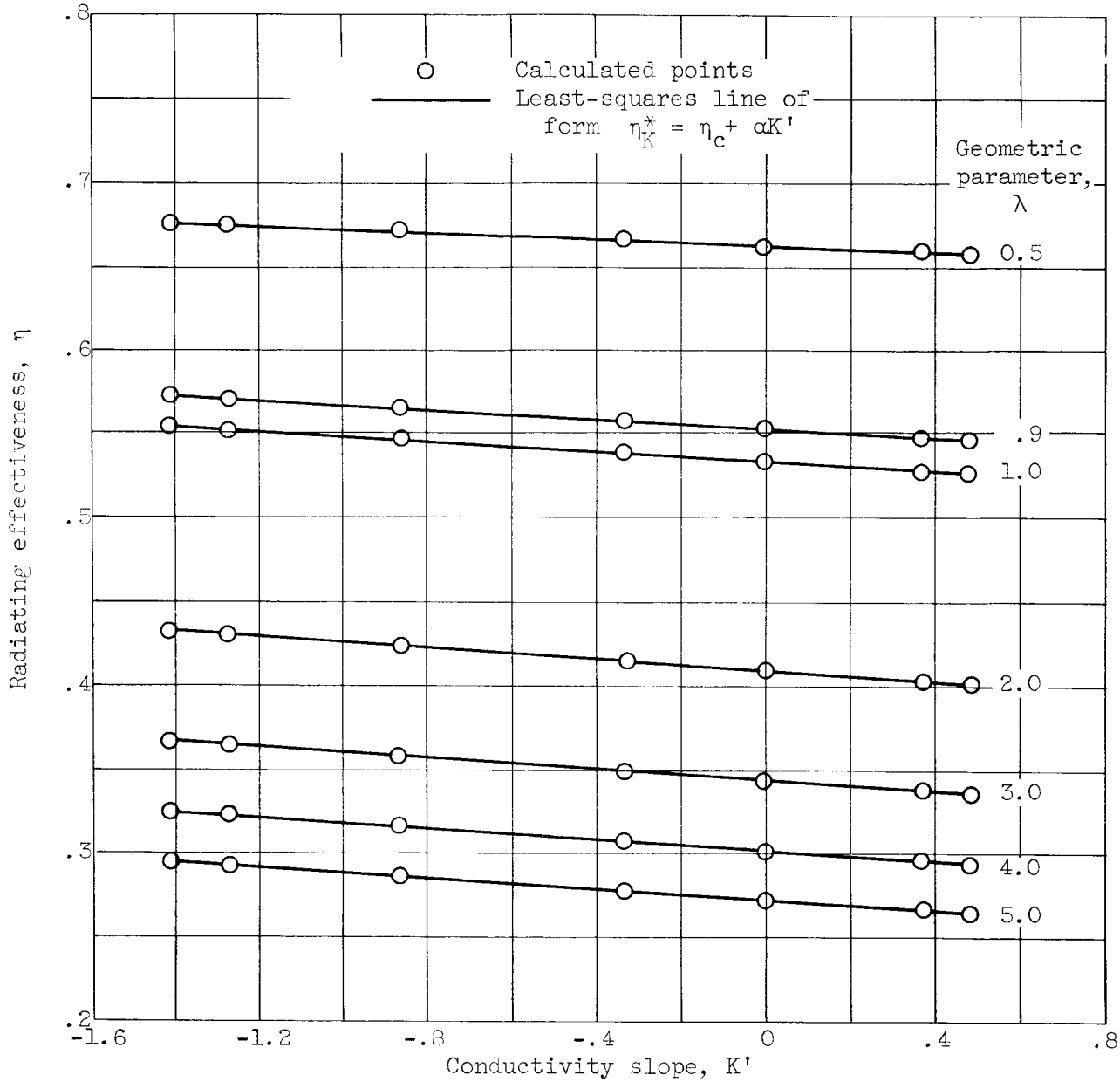

Figure 9. - Radiating effectiveness as a function of conductivity slope.

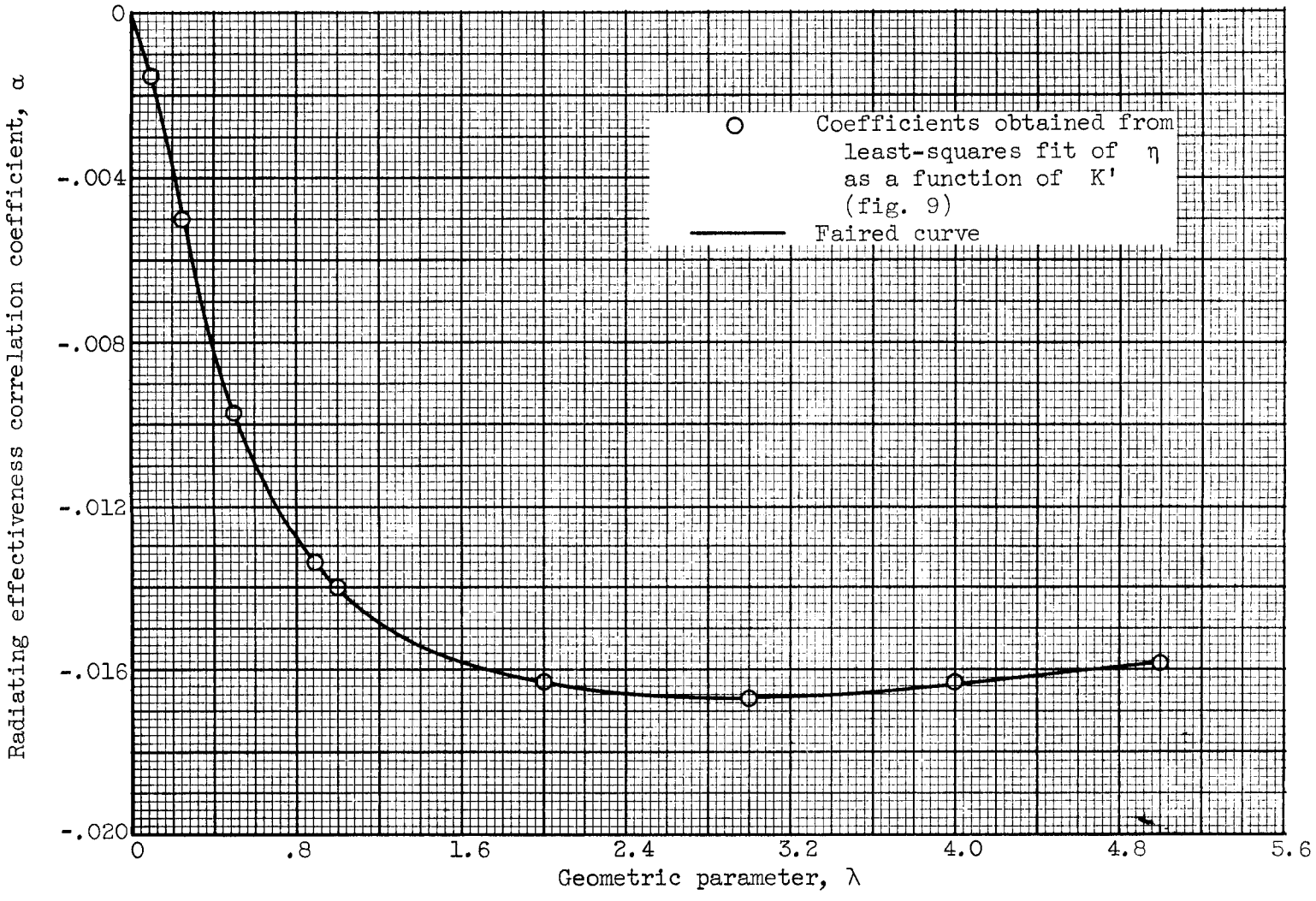

Figure 10. - Radiating effectiveness correlation coefficient as a function of geometric parameter for variable conductivity.

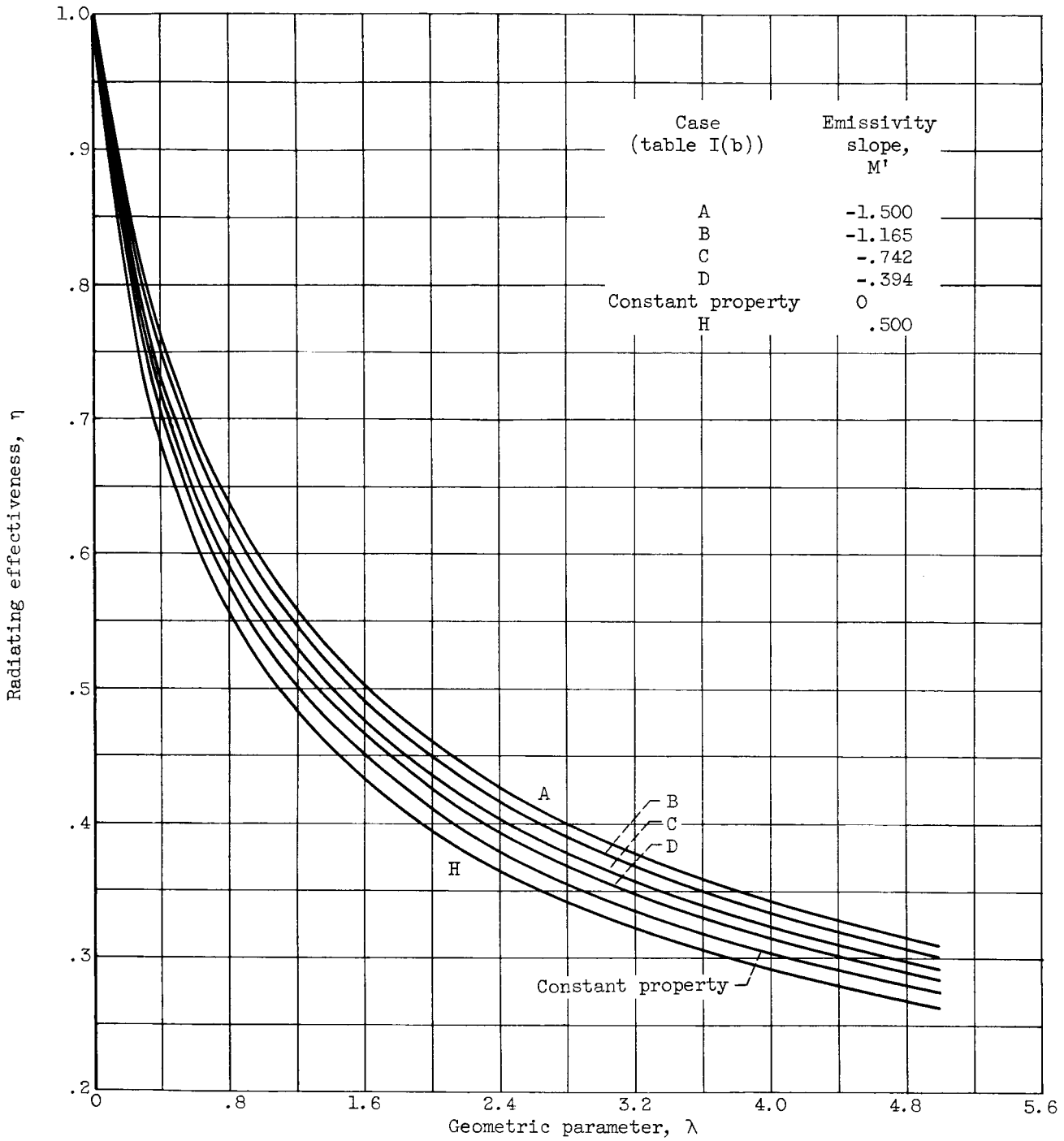

Figure 11. - Effect of variable emissivity on radiating effectiveness.

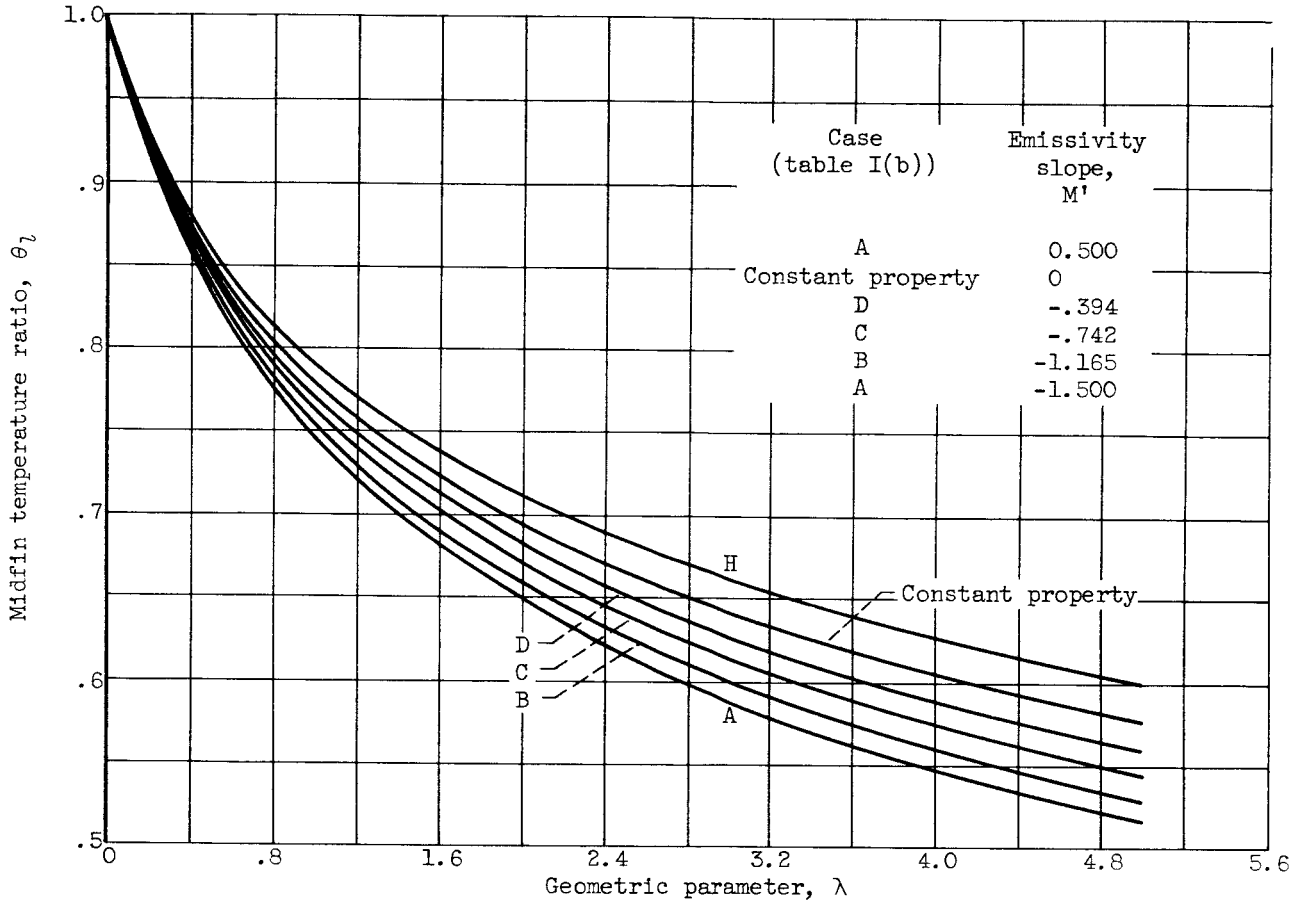

Figure 12. - Effect of variable emissivity on midfin temperature ratio.

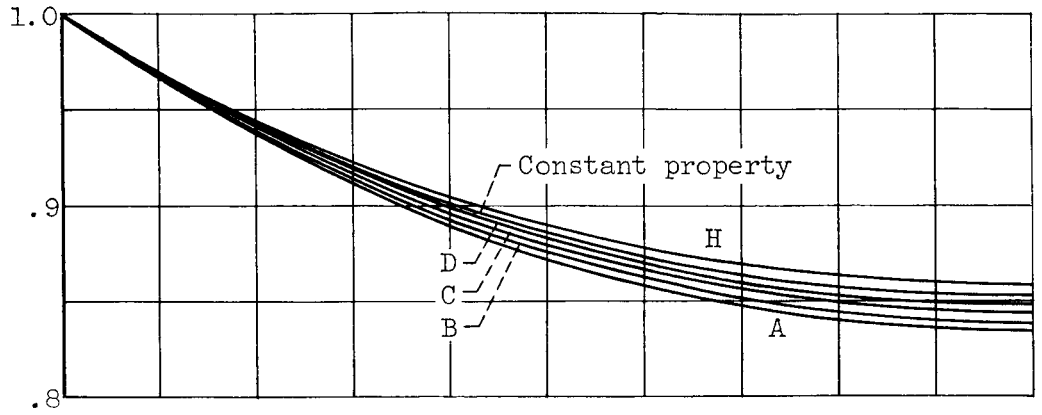

(a) Geometric parameter, λ, 0.5.

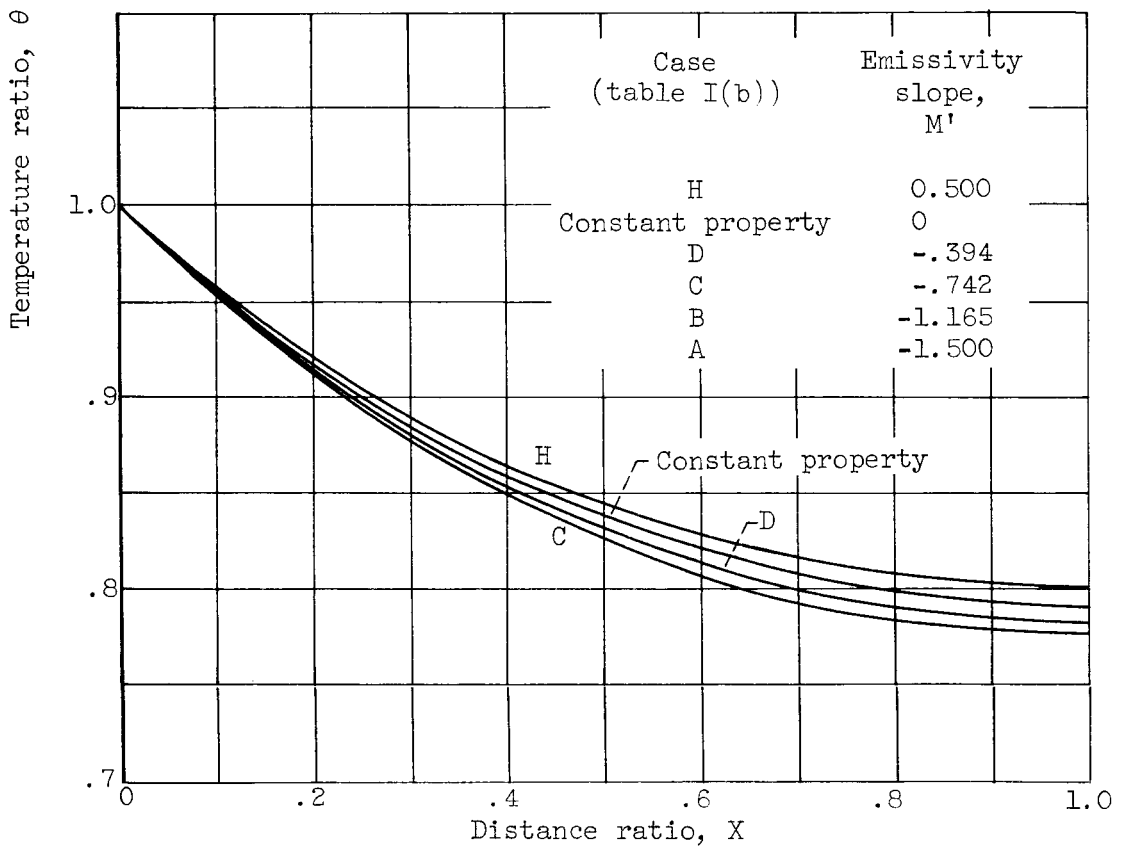

(b) Geometric parameter, λ, 0.9.

Figure 13. - Effect of variable emissivity on local temperature ratio.

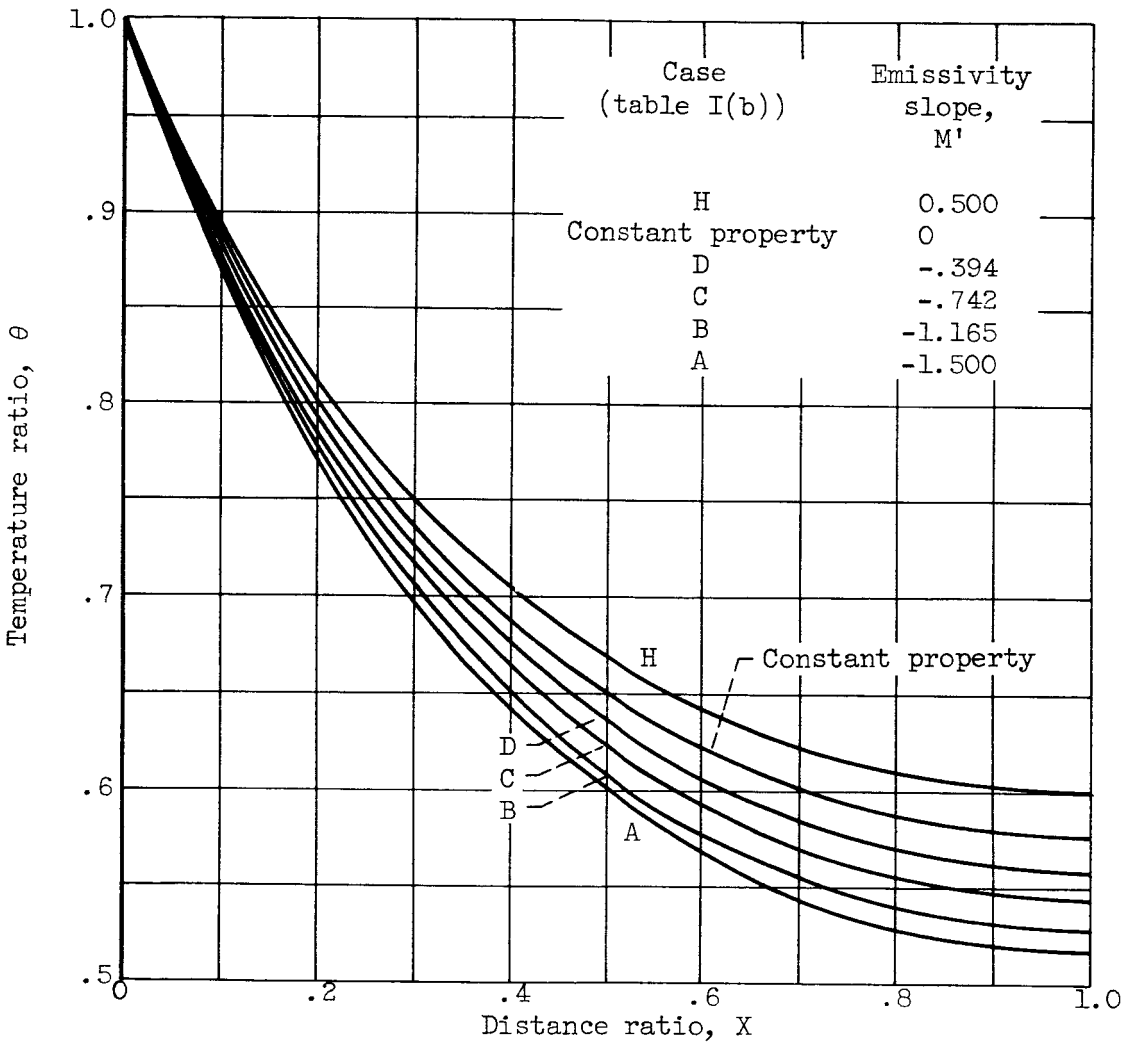

(c) Geometric parameter, λ, 5.0.

Figure 13. - Concluded. Effect of variable emissivity on local temperature ratio.

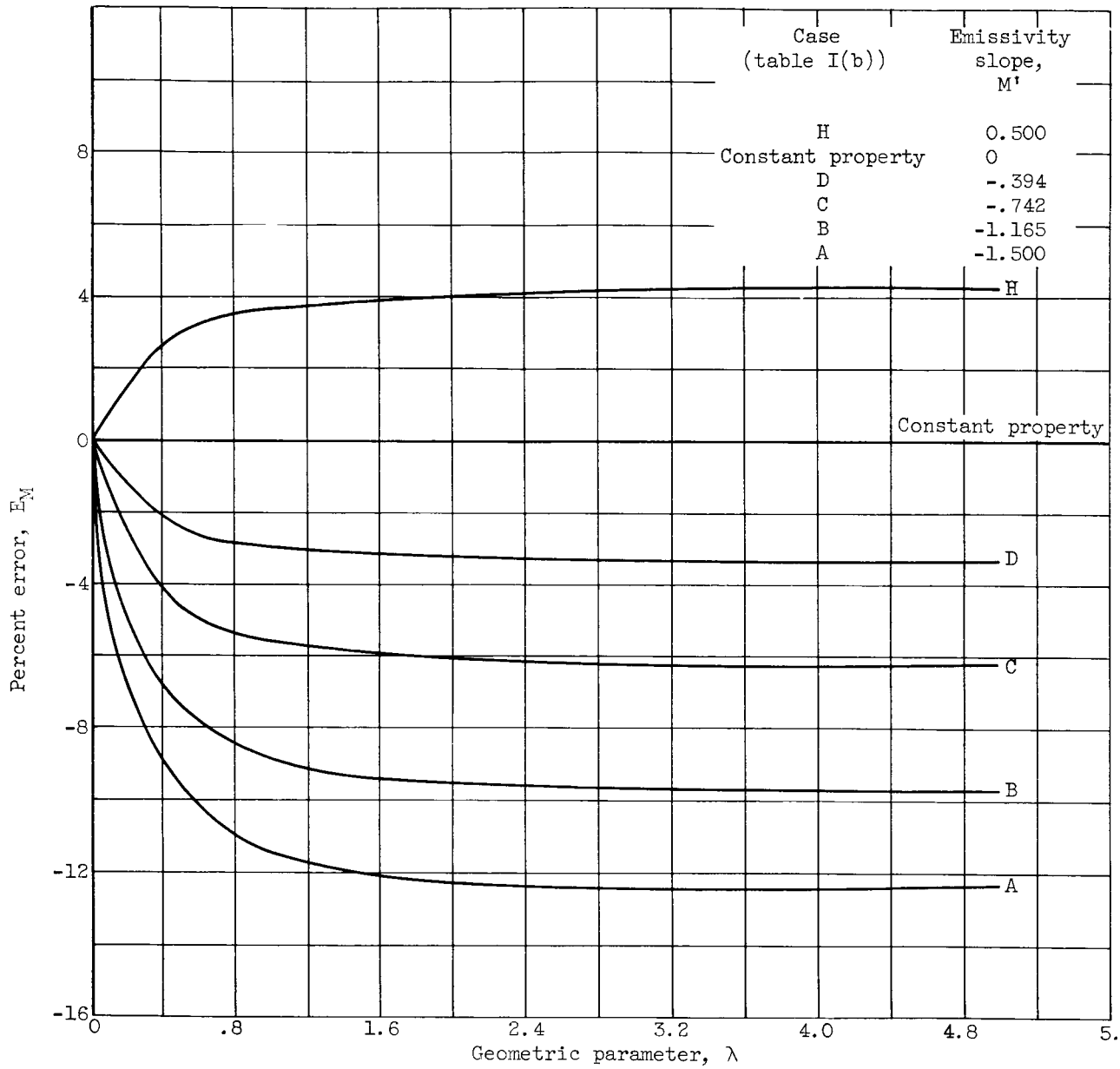

Figure 14. - Percent error in fin effectiveness for variable emissivity.

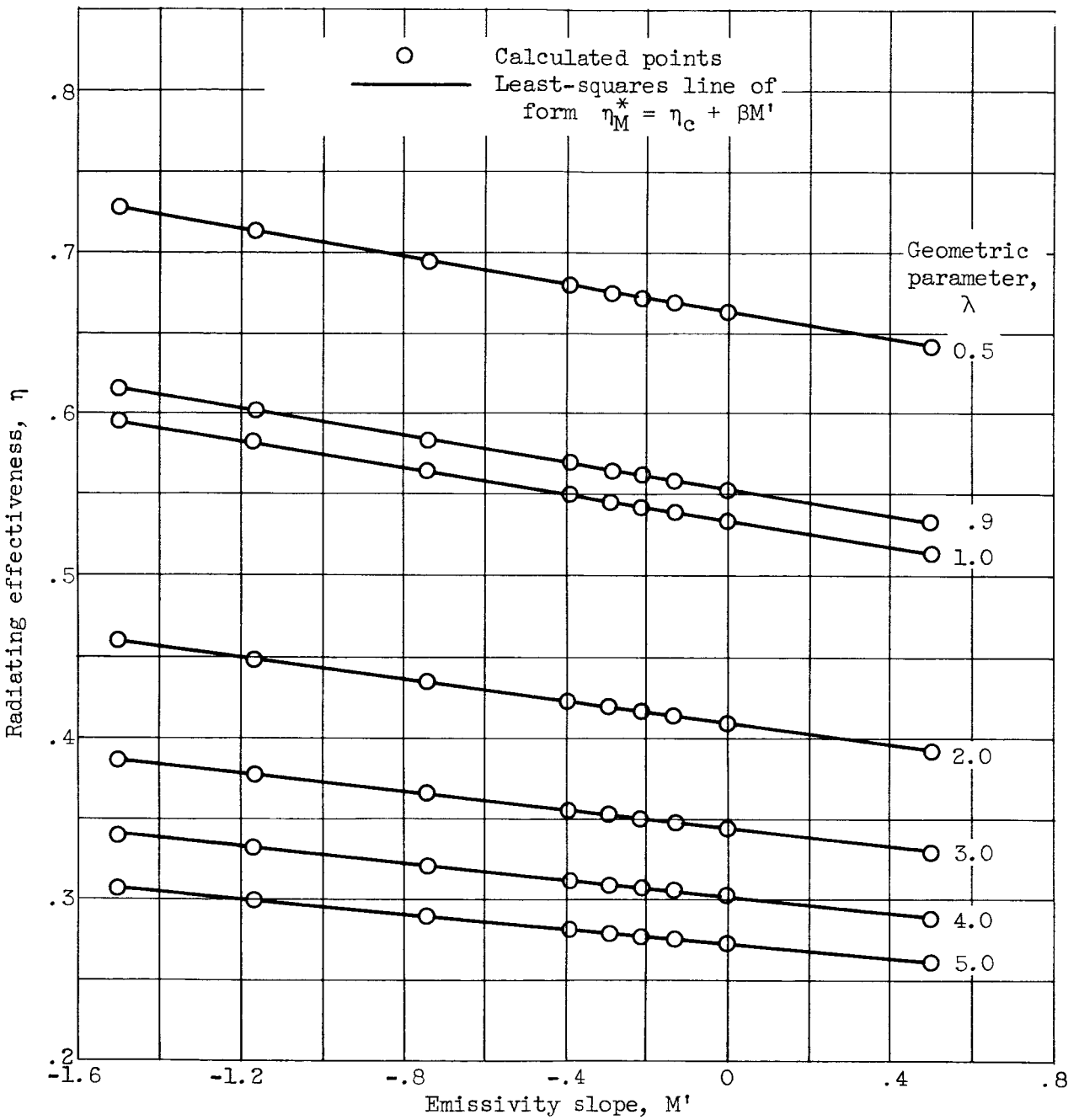

Figure 15. - Radiating effectiveness as a function of emissivity slope.

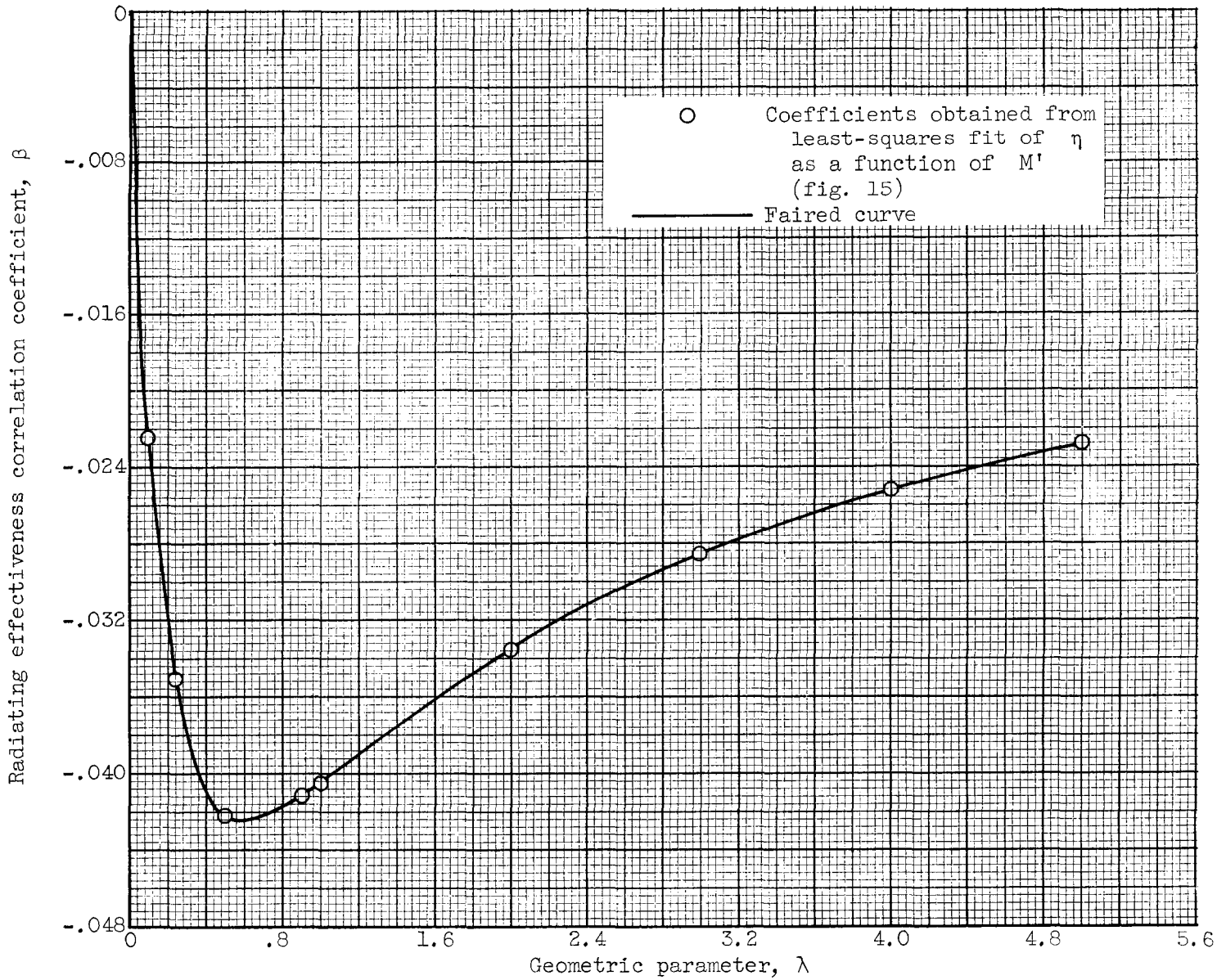

Figure 16. - Radiating effectiveness correlation coefficient as a function of geometric parameter for variable emissivity.

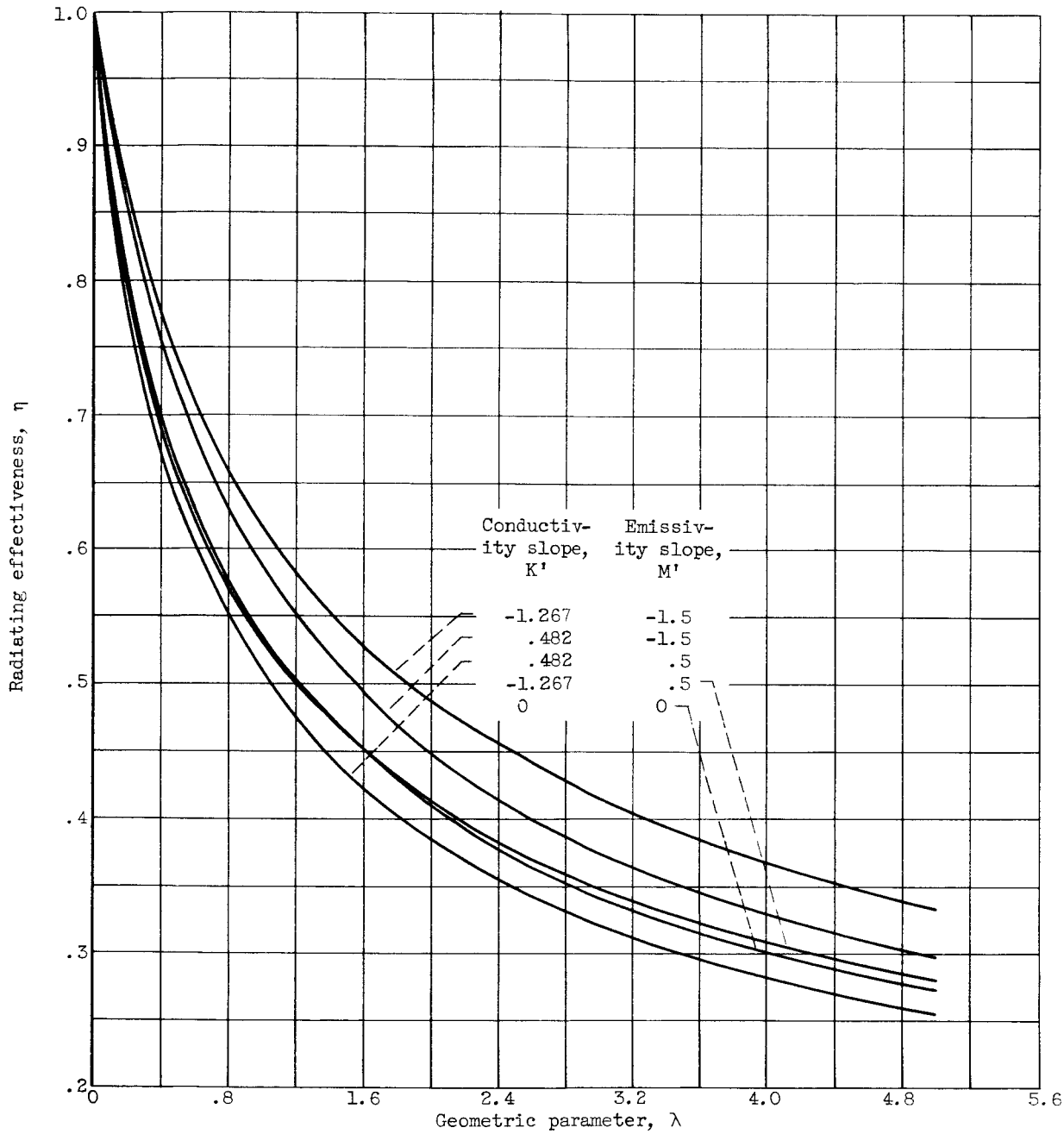

Figure 17. - Effect of variable conductivity and emissivity on radiating effectiveness.

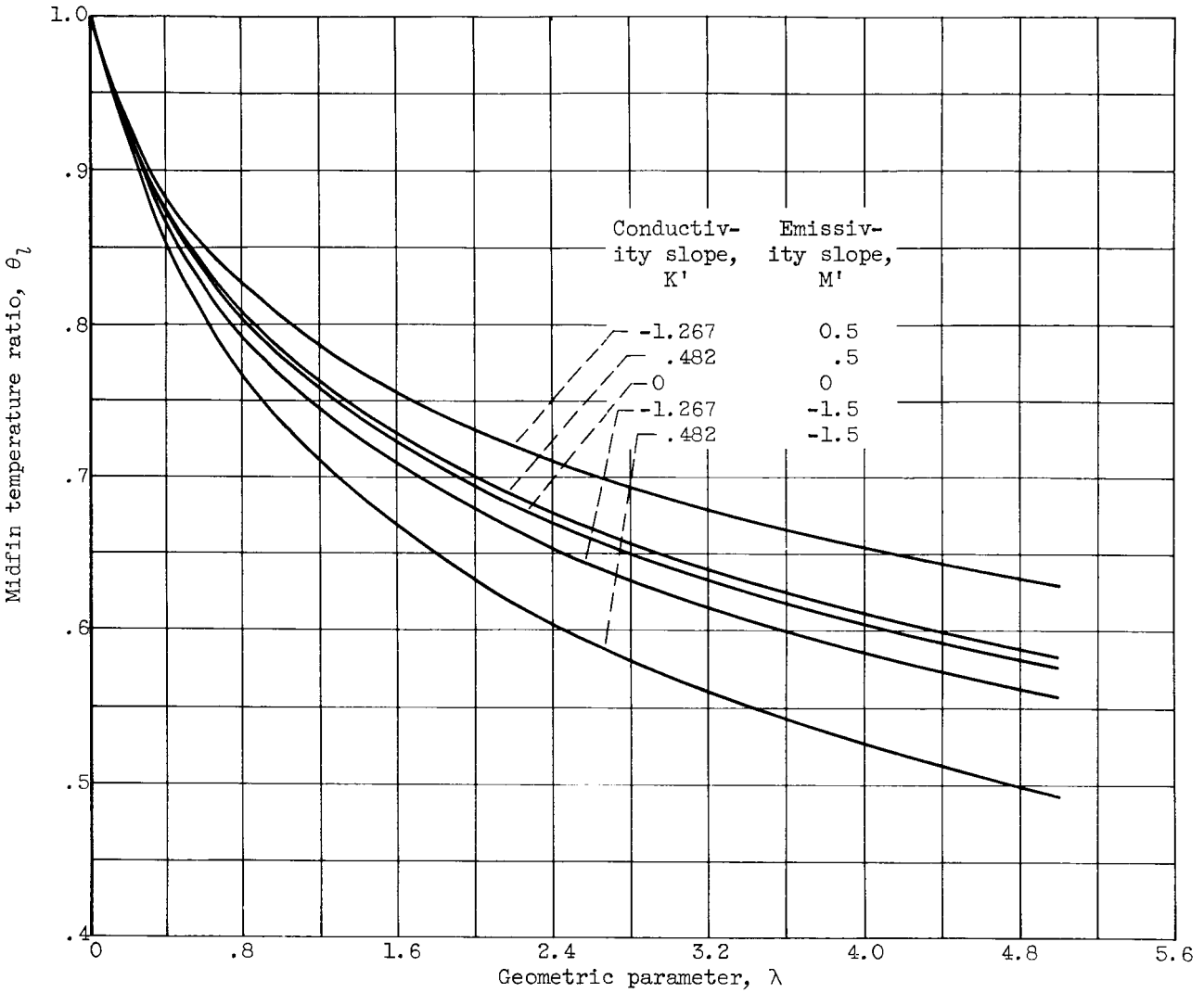

Figure 18. - Effect of variable conductivity and emissivity on midfin temperature ratio.

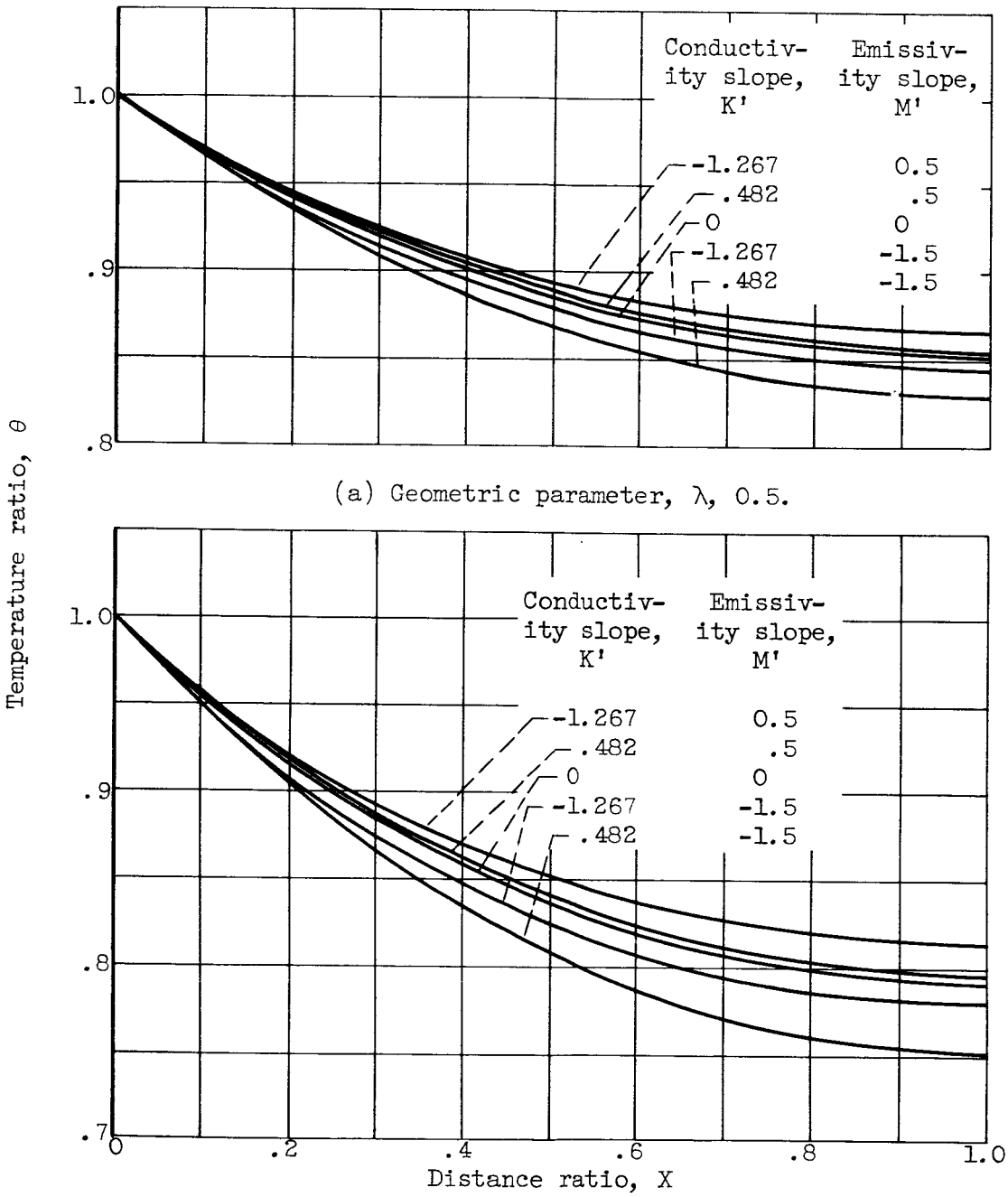

Figure 19. - Effect of variable conductivity and emissivity on local temperature ratio.

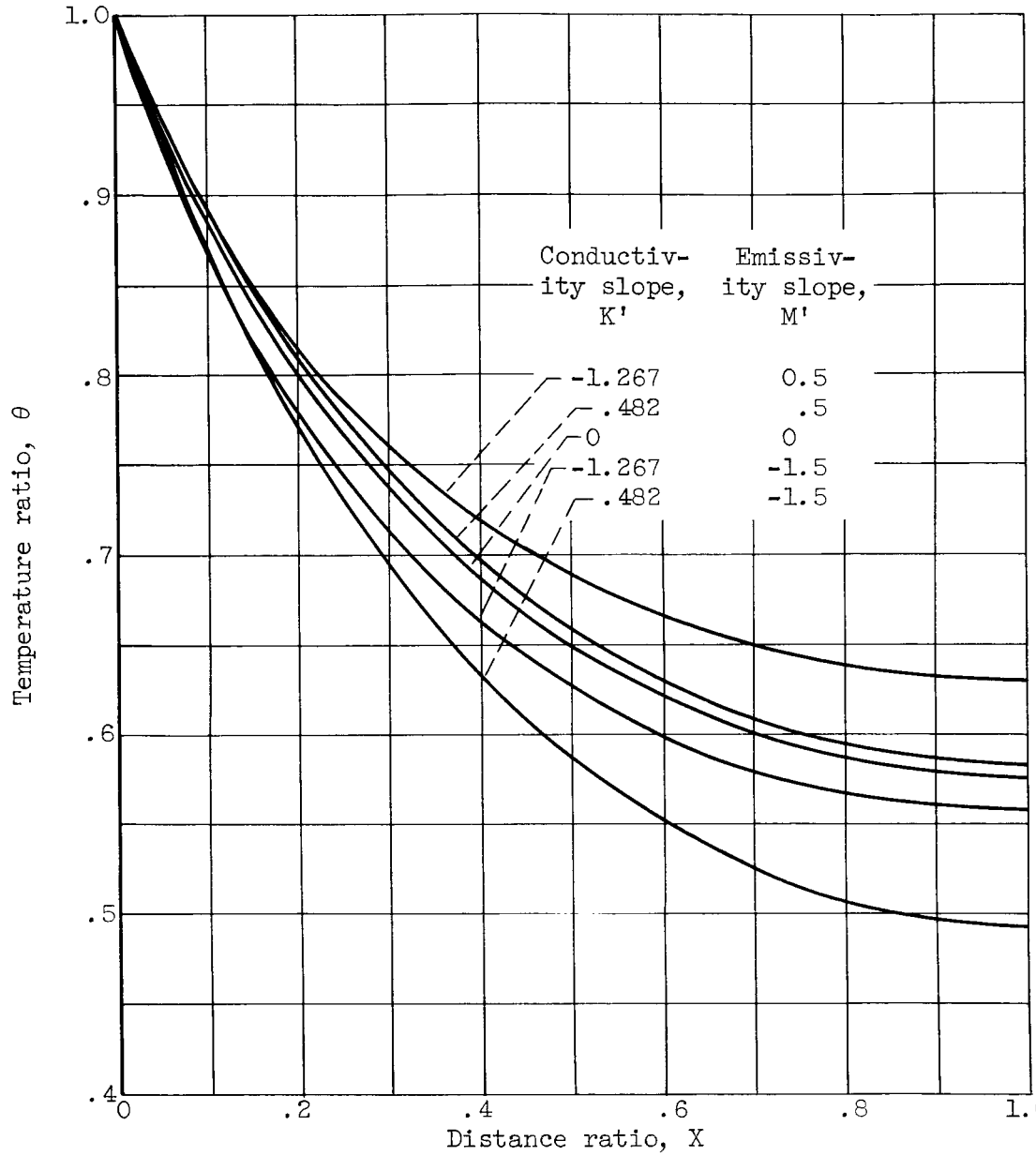

(c) Geometric parameter, λ, 5.0.

Figure 19. - Concluded. Effect of variable conductivity and emissivity on local temperature ratio.

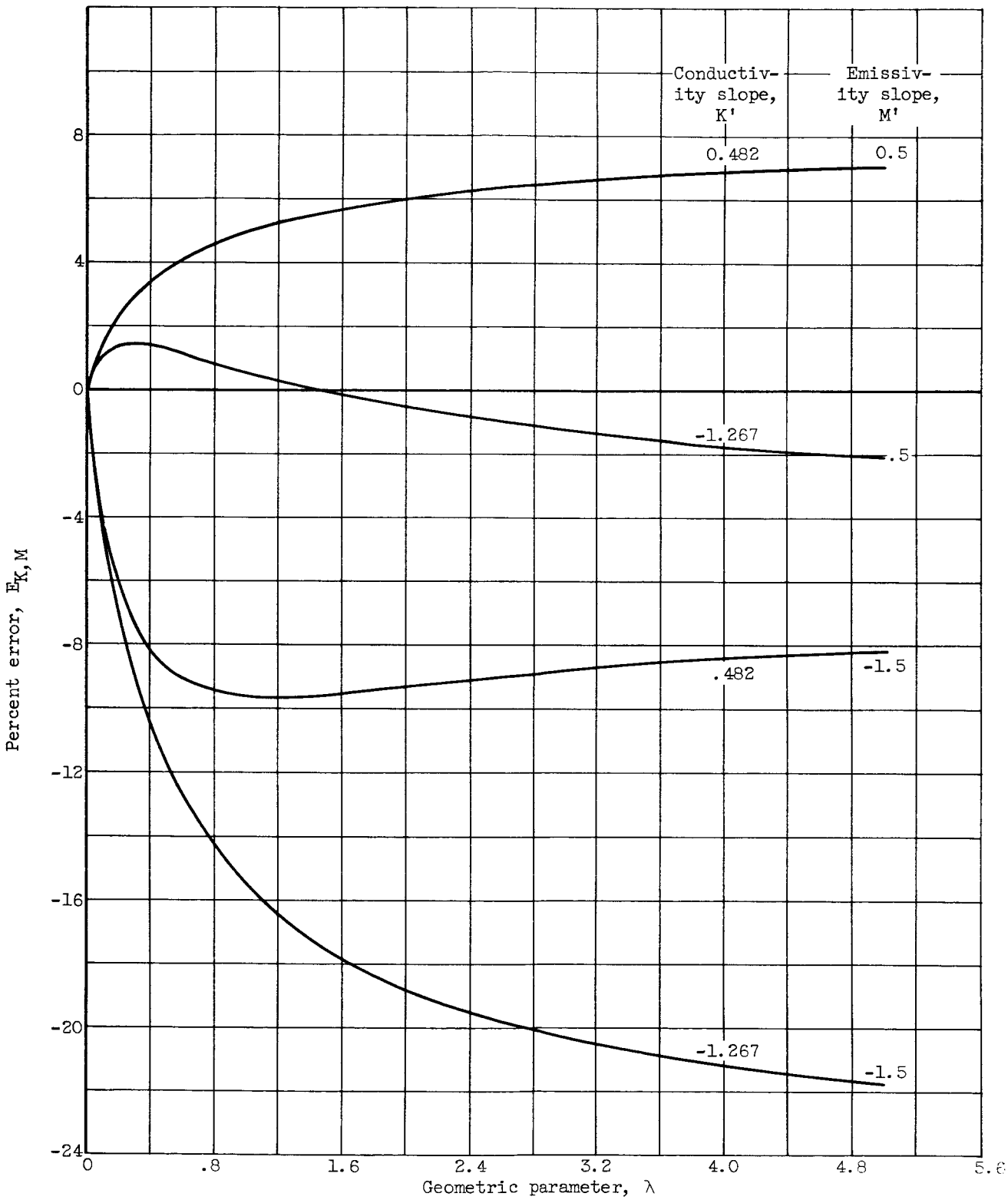

Figure 20. - Percent error in fin effectiveness for variable conductivity and emissivity.

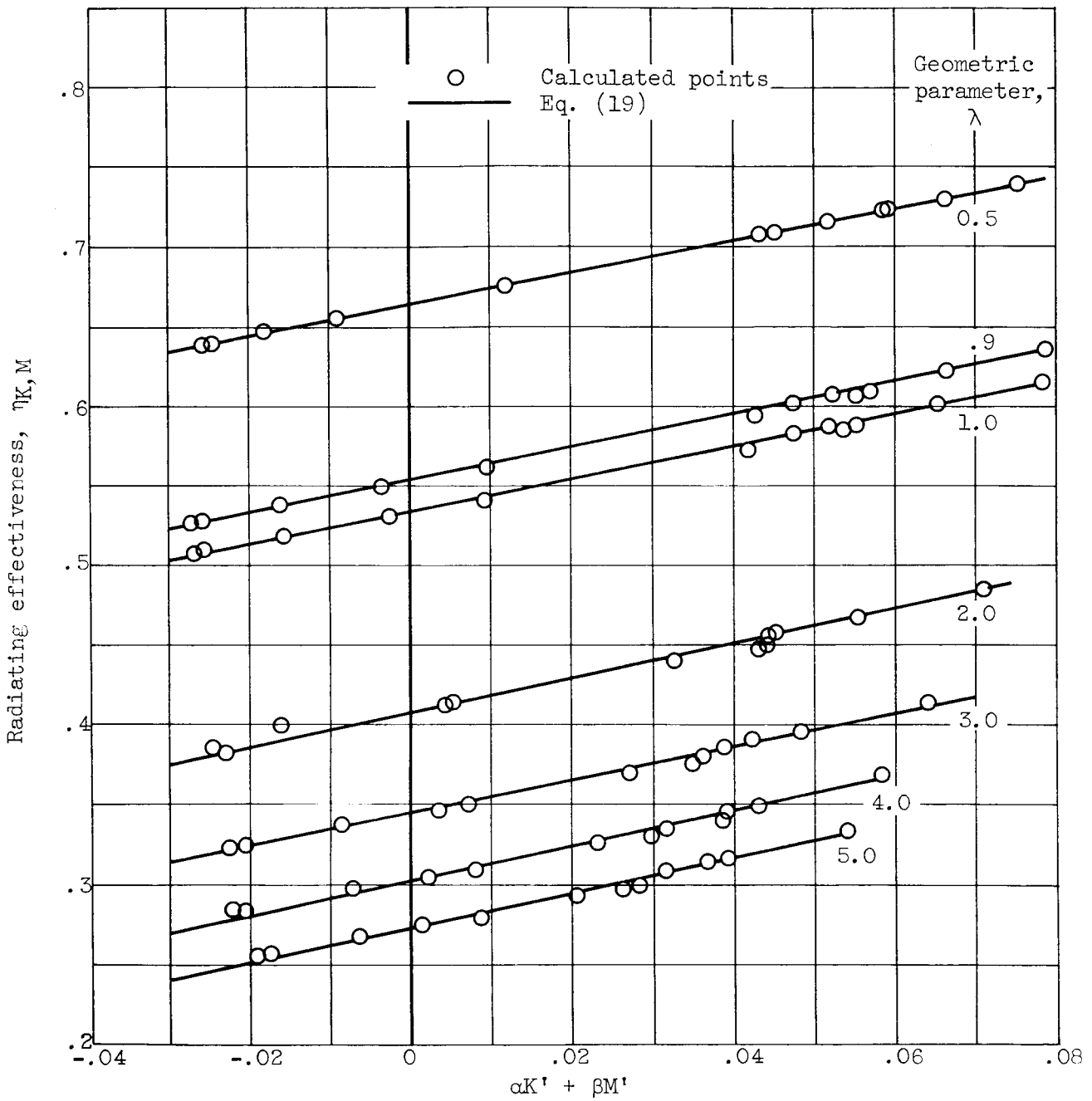

Figure 21. - Radiating effectiveness as a function of linear combination of conductivity and emissivity slopes.

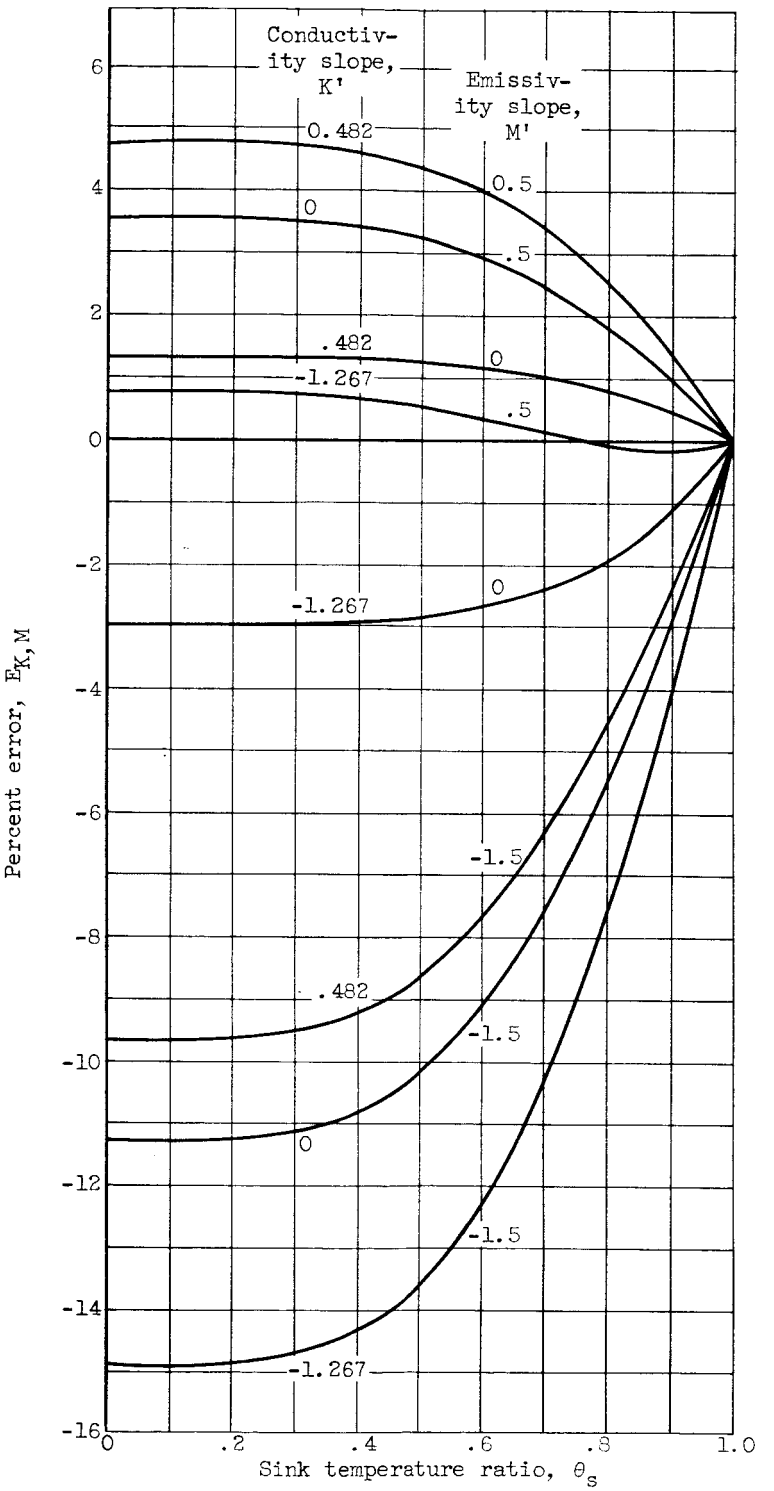

Figure 22. - Effect of nonzero sink temperature on percent error for several conductivity and emissivity variations. Geometric parameter. 0.9.